syndromic ichthyosis to chromosome 3q27-q28. J Invest Dermatol 2002;119:70-6.
106. Basel-Vanagaite L, Attia R, Ishida-Yamamoto A, Rainshtein L, Ben AD, Lurie R, et al. Autosomal recessive ichthyosis with hypotrichosis caused by a mutation in ST14, encoding type II transmembrane serine protease matriptase. Am J Hum Genet 2007;80:467-77.
107. Alef T, Torres S, Hausser I, Metze D, Tursen U, Lestringant GG, et al. Ichthyosis, follicular atrophoderma, and hypotrichosis caused by mutations in ST14 is associated with impaired profilaggrin processing. J Invest Dermatol 2009;129:862-9.
108. Lestringant GG, Kuster W, Frossard PM, Happle R. Congenital ichthyosis, follicular atrophoderma, hypotrichosis, and hypohidrosis: a new genodermatosis? Am J Med Genet 1998;75: 186-9.
109. Pujol RM, Moreno A, Alomar A, De Moragas JM. Congenital ichthyosiform dermatosis with linear keratotic flexural papules and sclerosing palmoplantar keratoderma. Arch Dermatol 1989;125:103-6.
110. Dahlqvist J, Klar J, Tiwari N, Schuster J, Torma H, Badhai J, et al. A single-nucleotide deletion in the POMP 5' UTR causes a transcriptional switch and altered epidermal proteasome distribution in KLICK genodermatosis. Am J Hum Genet 2010; 86:596-603.
111. Gottron H. Congenital angelegte symmetrische progressive erythrokderatodermie. Zentralbl Haut Geschlechtskrankh 1922;4:493-4.
112. Darier MJ. Erythro-kératodermie verruqueuse en nappes, symétrique et progressive. Bull Soc Fr Dermatol Syph 1911; 2:252-64.
113. Mendes da Costa S. Erythro- et keratodermia variabilis in a mother and daughter. Acta Derm Venereol 1925;6:255-61.
114. Richard G, Brown N, Rouan F, Van der Schroeff JG, Bijlsma E, Eichenfield LF, et al. Genetic heterogeneity in erythrokeratodermia variabilis: novel mutations in the connexin gene GJB4 (Cx30.3) and genotype-phenotype correlations. J Invest Dermatol 2003;120:601-9.
115. Richard G, Smith LE, Bailey RA, Itin P, Hohl D, Epstein EH Jr, et al. Mutations in the human connexin gene GJB3 cause erythrokeratodermia variabilis. Nat Genet 1998;20:366-9.
116. Macari F, Landau M, Cousin P, Mevorah B, Brenner S, Panizzon R, et al. Mutation in the gene for connexin 30.3 in a family with erythrokeratodermia variabilis. Am J Hum Genet 2000;67:1296-301.
117. van Steensel MA, Oranje AP, Van der Schroeff JG, Wagner A, van Geel M. The missense mutation G12D in connexin30.3 can cause both erythrokeratodermia variabilis of Mendes da Costa and progressive symmetric erythrokeratodermia of Gottron. Am J Med Genet A 2009;149A:657-61.
118. Burns FS. A case of generalized congenital keratoderma with unusual involvement of the eyes, ears, and nasal and buccous membranes. J Cutan Dis 1915;33:255-60.
119. Skinner BA, Greist MC, Norins AL. The keratitis, ichthyosis, and deafness (KID) syndrome. Arch Dermatol 1981;117:285-9.
120. Gulzow J, Anton-Lamprecht I. Ichthyosis hystrix gravior typus Rheydt: an otologic-dermatologic syndrome (Ichthyosis hystrix gravior Typus Rheydt: ein otologisch-dermatologisches Syndrom). Laryngol Rhinol Otol Stuttg 1977;56:949-55.
121. Richard G, Rouan F, Willoughby CE, Brown N, Chung P, Ryynanen M, et al. Missense mutations in GJB2 encoding connexin-26 cause the ectodermal dysplasia keratitis-ichthyosis-deafness syndrome. Am J Hum Genet 2002;70: 1341-8.
122. van Steensel MA, Steijlen PM, Bladergroen RS, Hoefsloot EH, van Ravenswaaij-Arts CM, van Geel M. A phenotype resembling the Clouston syndrome with deafness is associated with a novel missense GJB2 mutation. J Invest Dermatol 2004;123: 291-3.
123. Netherton EW. A unique case of trichorrhexis nodosa; bamboo hairs. AMA Arch Dermatol 1958;78:483-7.
124. Levy SB, Goldsmith LA. The peeling skin syndrome. J Am Acad Dermatol 1982;7:606-13.
125. Chavanas S, Bodemer C, Rochat A, Hamel-Teillac D, Ali M, Irvine AD, et al. Mutations in SPINK5, encoding a serine protease inhibitor, cause Netherton syndrome. Nat Genet 2000;25:141-2.
126. Komatsu N, Suga Y, Saijoh K, Liu AC, Khan S, Mizuno Y, et al. Elevated human tissue kallikrein levels in the stratum corneum and serum of peeling skin syndrome-type B patients suggests an over-desquamation of corneocytes. J Invest Dermatol 2006;126:2338-42.
127. Vohwinkel KH. Keratoma hereditarium mutilans. Arch Dermatol Syph 1929;158:354-64.
128. Maestrini E, Korge BP, Ocana-Sierra J, Calzolari E, Cambiaghi S, Scudder PM, et al. A missense mutation in connexin26, D66H, causes mutilating keratoderma with sensorineural deafness (Vohwinkel's syndrome) in three unrelated families. Hum Mol Genet 1999;8:1237-43.
129. Stulli L. Di una variata cutanea. Lettera al direttore dell'Antologia. Estratti dall Antologia di Firence 1826;71-72:1-3.
130. Fischer J, Bouadjar B, Heilig R, Huber M, Lefevre C, Jobard F, et al. Mutations in the gene encoding SLURP-1 in Mal de Meleda. Hum Mol Genet 2001;10:875-80.
131. Papillon M, Lefèvre P. Deux cas de kératodermie palmaire et plantaire symétrique familiale (maladie de Meleda) chez le frère et la soeur. Coexistence dans les deux cas d'altérations dentaires graves. Bull Soc Fr Dermatol Syph 1924;31:82-7.
132. Toomes C, James J, Wood AJ, Wu CL, McCormick D, Lench N, et al. Loss-of-function mutations in the cathepsin C gene result in periodontal disease and palmoplantar keratosis. Nat Genet 1999;23:421-4.
133. Coulombe PA, Hutton ME, Letai A, Hebert A, Paller AS, Fuchs E. Point mutations in human keratin 14 genes of epidermolysis bullosa simplex patients: genetic and functional analyses. Cell 1991;66:1301-11.
134. Lane EB, Rugg EL, Navsaria H, Leigh IM, Heagerty AH, Ishida-Yamamoto A, et al. A mutation in the conserved helix termination peptide of keratin 5 in hereditary skin blistering. Nature 1992;356:244-6.
135. Fine JD, Eady RA, Bauer EA, Bauer JW, Bruckner-Tuderman L, Heagerty A, et al. The classification of inherited epidermolysis bullosa (EB): report of the third international consensus meeting on diagnosis and classification of EB. J Am Acad Dermatol 2008;58:931-50.
136. Haenssle HA, Finkenrath A, Hausser I, Oji V, Traupe H, Hennies HC, et al. Effective treatment of severe thermodysregulation by oral retinoids in a patient with recessive congenital lamellar ichthyosis. Clin Exp Dermatol 2008;33:578-81.
137. DiGiovanna JJ, Priolo M, Itin P. Approach towards a new classification for ectodermal dysplasias: integration of the clinical and molecular knowledge. Am J Med Genet A 2009; 149A:2068-70.
138. Salinas CF, Jorgenson RJ, Wright JT, DiGiovanna JJ, Fete MD. 2008 International conference on ectodermal dysplasias classification: conference report. Am J Med Genet A 2009; 149A:1958-69.
139. Plantin P, Gavanou J, Jouan N, Leroy JP, Guillet G. Collodion skin: a misdiagnosed but frequent clinical aspect of anhidrotic ectodermal dysplasia during the neonatal period (Peau collodionnée: un aspect clinique méconnu mais fréquent des

dysplasies ectodermiques anhidrotiques en période néonatale). Ann Dermatol Venereol 1992;119:821-3.
140. Thomas C, Suranyi E, Pride H, Tyler W. A child with hypohidrotic ectodermal dysplasia with features of a collodion membrane. Pediatr Dermatol 2006;23:251-4.
141. Navarro CL, De Sandre-Giovannoli A, Bernard R, Boccaccio I, Boyer A, Genevieve D, et al. Lamin A and ZMPSTE24 (FACE-1) defects cause nuclear disorganization and identify restrictive dermopathy as a lethal neonatal laminopathy. Hum Mol Genet 2004;13:2493-503.
142. Lowry RB, Machin GA, Morgan K, Mayock D, Marx L. Congenital contractures, edema, hyperkeratosis, and intrauterine growth retardation: a fatal syndrome in Hutterite and Mennonite kindreds. Am J Med Genet 1985;22:531-43.
143. Antoine T. Ein Fall von allgemeiner, angeborener Hautatrophie. Monatsschr Geburtsh Gynaekol 1929;81:276-83.
144. Manning MA, Cunniff CM, Colby CE, El-Sayed YY, Hoyme HE. Neu-Laxova syndrome: detailed prenatal diagnostic and post-mortem findings and literature review. Am J Med Genet A 2004;125A:240-9.
145. Happle R, Koch H, Lenz W. The CHILD syndrome: congenital hemidysplasia with ichthyosiform erythroderma and limb defects. Eur J Pediatr 1980;134:27-33.
146. Konig A, Happle R, Bornholdt D, Engel H, Grzeschik KH. Mutations in the NSDHL gene, encoding a 3beta-hydroxysteroid dehydrogenase, cause CHILD syndrome. Am J Med Genet 2000;90:339-46.
147. Happle R, Matthiass HH, Macher E. Sex-linked chondrodysplasia punctata? Clin Genet 1977;11:73-6.
148. Darier J. Psorospermose folliculaire végétante. Ann Dermatol Syph 1889;10:597-612.
149. White J. A case of keratosis (ichthyosis) follicularis. J Cutan Dis 1889;7:201-9.
150. Hailey H, Hailey H. Familial benign chronic pemphigus. Arch Dermatol Syph 1939;39:679-85.
151. Sakuntabhai A, Ruiz-Perez V, Carter S, Jacobsen N, Burge S, Monk S, et al. Mutations in ATP2A2, encoding a $Ca2^{+}$ pump, cause Darier disease. Nat Genet 1999;21:271-7.
152. Hu Z, Bonifas JM, Beech J, Bench G, Shigihara T, Ogawa H, et al. Mutations in ATP2C1, encoding a calcium pump, cause Hailey-Hailey disease. Nat Genet 2000;24:61-5.
153. Madison KC. Barrier function of the skin: "la raison d'etre" of the epidermis. J Invest Dermatol 2003;121:231-41.
154. Attenborough D. Life on earth. Boston: Little Brown; 1980.
155. Blank IH. Further observations on factors which influence the water content of the stratum corneum. J Invest Dermatol 1953;21:259-71.
156. Winsor T, Burge GE. Differential roles of layers of human epigastric skin on diffusion rate of water. Arch Intern Med 1944;74:428-36.
157. Elias PM. Epidermal lipids, barrier function, and desquamation. J Invest Dermatol 1983;80:44-49s.
158. Williams ML. The ichthyoses—pathogenesis and prenatal diagnosis: a review of recent advances. Pediatr Dermatol 1983;1:1-24.
159. Demerjian M, Crumrine DA, Milstone LM, Williams ML, Elias PM. Barrier dysfunction and pathogenesis of neutral lipid storage disease with ichthyosis (Chanarin-Dorfman syndrome). J Invest Dermatol 2006;126:2032-8.
160. Elias PM, Schmuth M, Uchida Y, Rice RH, Behne M, Crumrine D, et al. Basis for the permeability barrier abnormality in lamellar ichthyosis. Exp Dermatol 2002;11:248-56.
161. Elias PM, Crumrine D, Rassner U, Hachem JP, Menon GK, Man W, et al. Basis for abnormal desquamation and permeability barrier dysfunction in RXLI. J Invest Dermatol 2004;122:314-9.
162. Hachem JP, Houben E, Crumrine D, Man MQ, Schurer N, Roelandt T, et al. Serine protease signaling of epidermal permeability barrier homeostasis. J Invest Dermatol 2006;126:2074-86.
163. Holleran WM, Ginns EI, Menon GK, Grundmann JU, Fartasch M, McKinney CE, et al. Consequences of beta-glucocerebrosidase deficiency in epidermis: ultrastructure and permeability barrier alterations in Gaucher disease. J Clin Invest 1994;93:1756-64.
164. Schmuth M, Fluhr JW, Crumrine DC, Uchida Y, Hachem JP, Behne M, et al. Structural and functional consequences of loricrin mutations in human loricrin keratoderma (Vohwinkel syndrome with ichthyosis). J Invest Dermatol 2004;122:909-22.
165. Descargues P, Deraison C, Bonnart C, Kreft M, Kishibe M, Ishida-Yamamoto A, et al. Spink5-deficient mice mimic Netherton syndrome through degradation of desmoglein 1 by epidermal protease hyperactivity. Nat Genet 2005;37:56-65.
166. Yanagi T, Akiyama M, Nishihara H, Sakai K, Nishie W, Tanaka S, et al. Harlequin ichthyosis model mouse reveals alveolar collapse and severe fetal skin barrier defects. Hum Mol Genet 2008;17:3075-83.
167. Matsuki M, Yamashita F, Ishida-Yamamoto A, Yamada K, Kinoshita C, Fushiki S, et al. Defective stratum corneum and early neonatal death in mice lacking the gene for transglutaminase 1 (keratinocyte transglutaminase). Proc Natl Acad Sci U S A 1998;95:1044-9.
168. Epp N, Furstenberger G, Muller K, de Juanes S, Leitges M, Hausser I, et al. 12R-lipoxygenase deficiency disrupts epidermal barrier function. J Cell Biol 2007;177:173-82.
169. Furuse M, Hata M, Furuse K, Yoshida Y, Haratake A, Sugitani Y, et al. Claudin-based tight junctions are crucial for the mammalian epidermal barrier: a lesson from claudin-1-deficient mice. J Cell Biol 2002;156:1099-111.
170. Feingold KR. The regulation of epidermal lipid synthesis by permeability barrier requirements. Crit Rev Ther Drug Carrier Syst 1991;8:193-210.
171. Ghadially R, Brown BE, Sequeira-Martin SM, Feingold KR, Elias PM. The aged epidermal permeability barrier: structural, functional, and lipid biochemical abnormalities in humans and a senescent murine model. J Clin Invest 1995;95:2281-90.
172. Williams ML, Elias PM. From basket weave to barrier: unifying concepts for the pathogenesis of the disorders of cornification. Arch Dermatol 1993;129:626-9.
173. Juanes SD, Epp N, Latzko S, Neumann M, Furstenberger G, Hausser I, et al. Development of an ichthyosiform phenotype in Alox12b-deficient mouse skin transplants. J Invest Dermatol 2009;129:1429-36.
174. Ballabio A, Parenti G, Carrozzo R, Sebastio G, Andria G, Buckle V, et al. Isolation and characterization of a steroid sulfatase cDNA clone: genomic deletions in patients with X-chromosome-linked ichthyosis. Proc Natl Acad Sci U S A 1987;84:4519-23.
175. Chipev CC, Korge BP, Markova N, Bale SJ, DiGiovanna JJ, Compton JG, et al. A leucine—proline mutation in the H1 subdomain of keratin 1 causes epidermolytic hyperkeratosis. Cell 1992;70:821-8.
176. Compton JG, DiGiovanna JJ, Santucci SK, Kearns KS, Amos CI, Abangan DL, et al. Linkage of epidermolytic hyperkeratosis to the type II keratin gene cluster on chromosome 12q. Nat Genet 1992;1:301-5.
177. Grzeschik KH, Bornholdt D, Oeffner F, Konig A, del Carmen BM, Enders H, et al. Deficiency of PORCN, a regulator of Wnt

signaling, is associated with focal dermal hypoplasia. Nat Genet 2007;39:833-5.
178. Jansen GA, Ofman R, Ferdinandusse S, Ijlst L, Muijsers AO, Skjeldal OH, et al. Refsum disease is caused by mutations in the phytanoyl-CoA hydroxylase gene. Nat Genet 1997;17:190-3.
179. Jansen GA, Waterham HR, Wanders RJ. Molecular basis of Refsum disease: sequence variations in phytanoyl-CoA hydroxylase (PHYH) and the PTS2 receptor (PEX7). Hum Mutat 2004;23:209-18.
180. Oeffner F, Fischer G, Happle R, Konig A, Betz RC, Bornholdt D, et al. IFAP syndrome is caused by deficiency in MBTPS2, an intramembrane zinc metalloprotease essential for cholesterol homeostasis and ER stress response. Am J Hum Genet 2009; 84:459-67.
181. Rothnagel JA, Dominey AM, Dempsey LD, Longley MA, Greenhalgh DA, Gagne TA, et al. Mutations in the rod domains of keratins 1 and 10 in epidermolytic hyperkeratosis. Science 1992;257:1128-30.
182. Rothnagel JA, Traupe H, Wojcik S, Huber M, Hohl D, Pittelkow MR, et al. Mutations in the rod domain of keratin 2e in patients with ichthyosis bullosa of Siemens. Nat Genet 1994; 7:485-90.
183. Smith FJ, Irvine AD, Terron-Kwiatkowski A, Sandilands A, Campbell LE, Zhao Y, et al. Loss-of-function mutations in the gene encoding filaggrin cause ichthyosis vulgaris. Nat Genet 2006;38:337-42.
184. Stefanini M, Lagomarsini P, Giliani S, Nardo T, Botta E, Peserico A, et al. Genetic heterogeneity of the excision repair defect associated with trichothiodystrophy. Carcinogenesis 1993;14:1101-5.
185. Takayama K, Salazar EP, Broughton BC, Lehmann AR, Sarasin A, Thompson LH, et al. Defects in the DNA repair and transcription gene ERCC2(XPD) in trichothiodystrophy. Am J Hum Genet 1996;58:263-70.
186. Tsuji S, Choudary PV, Martin BM, Stubblefield BK, Mayor JA, Barranger JA, et al. A mutation in the human glucocerebrosidase gene in neuronopathic Gaucher's disease. N Engl J Med 1987;316:570-5.
187. Mizrachi-Koren M, Shemer S, Morgan M, Indelman M, Khamaysi Z, Petronius D, et al. Homozygosity mapping as a screening tool for the molecular diagnosis of hereditary skin diseases in consanguineous populations. J Am Acad Dermatol 2006;55:393-401.
188. Lugassy J, Hennies HC, Indelman M, Khamaysi Z, Bergman R, Sprecher E. Rapid detection of homozygous mutations in congenital recessive ichthyosis. Arch Dermatol Res 2008;300: 81-5.
189. Roop D. Defects in the barrier. Science 1995;267:474-5.
190. Bitoun E, Bodemer C, Amiel J, de Prost Y, Stoll C, Calvas P, et al. Prenatal diagnosis of a lethal form of Netherton syndrome by SPINK5 mutation analysis. Prenat Diagn 2002;22:121-6.
191. Muller FB, Hausser I, Berg D, Casper C, Maiwald R, Jung A, et al. Genetic analysis of a severe case of Netherton syndrome and application for prenatal testing. Br J Dermatol 2002;146:495-9.
192. Sprecher E, Chavanas S, DiGiovanna JJ, Amin S, Nielsen K, Prendiville JS, et al. The spectrum of pathogenic mutations in SPINK5 in 19 families with Netherton syndrome: implications for mutation detection and first case of prenatal diagnosis. J Invest Dermatol 2001;117:179-87.
193. Rothnagel JA, Longley MA, Holder RA, Kuster W, Roop DR. Prenatal diagnosis of epidermolytic hyperkeratosis by direct gene sequencing. J Invest Dermatol 1994;102:13-6.
194. Rothnagel JA, Lin MT, Longley MA, Holder RA, Hazen PG, Levy ML, et al. Prenatal diagnosis for keratin mutations to exclude transmission of epidermolytic hyperkeratosis. Prenat Diagn 1998;18:826-30.
195. Tsuji-Abe Y, Akiyama M, Nakamura H, Takizawa Y, Sawamura D, Matsunaga K, et al. DNA-based prenatal exclusion of bullous congenital ichthyosiform erythroderma at the early stage, 10 to 11 weeks' of pregnancy, in two consequent siblings. J Am Acad Dermatol 2004;51:1008-11.
196. Sillen A, Holmgren G, Wadelius C. First prenatal diagnosis by mutation analysis in a family with Sjögren-Larsson syndrome. Prenat Diagn 1997;17:1147-9.
197. Yanagi T, Akiyama M, Sakai K, Nagasaki A, Ozawa N, Kosaki R, et al. DNA-based prenatal exclusion of harlequin ichthyosis. J Am Acad Dermatol 2008;58:653-6.
198. Akiyama M, Titeux M, Sakai K, McMillan JR, Tonasso L, Calvas P, et al. DNA-based prenatal diagnosis of harlequin ichthyosis and characterization of ABCA12 mutation consequences. J Invest Dermatol 2007;127:568-73.
199. Anton-Lamprecht I. The skin. In: Papdimitriou JM, Henderon DW, Sagnolo DV, editors. Diagnostic ultrastructure of non-neoplastic diseases: diagnostic ultrastructure of non-neoplastic diseases. Edinburgh: Churchill-Livingstone; 1992. pp. 459-550.
200. Anton-Lamprecht I. Ultrastructural identification of basic abnormalities as clues to genetic disorders of the epidermis. J Invest Dermatol 1994;103:6-12S.
201. Anton-Lamprecht I, Schnyder UW. Ultrastructural distinction of autosomal dominant ichthyosis vulgaris and X-linked recessive ichthyosis. Clin Genet 1976;10:245-7.
202. Oji V, Seller N, Sandilands A, Gruber R, Gerss J, Huffmeier U, et al. Ichthyosis vulgaris: novel FLG mutations in the German population and high presence of $CD1a^+$ cells in the epidermis of the atopic subgroup. Br J Dermatol 2009;160:771-81.
203. Dale BA, Holbrook KA, Fleckman P, Kimball JR, Brumbaugh S, Sybert VP. Heterogeneity in harlequin ichthyosis, an inborn error of epidermal keratinization: variable morphology and structural protein expression and a defect in lamellar granules. J Invest Dermatol 1990;94:6-18.
204. Akiyama M, Sakai K, Sato T, McMillan JR, Goto M, Sawamura D, et al. Compound heterozygous ABCA12 mutations including a novel nonsense mutation underlie harlequin ichthyosis. Dermatology 2007;215:155-9.
205. Ishida-Yamamoto A. Loricrin keratoderma: a novel disease entity characterized by nuclear accumulation of mutant loricrin. J Dermatol Sci 2003;31:3-8.
206. Arnold ML, Anton-Lamprecht I, Melz-Rothfuss B, Hartschuh W. Ichthyosis congenita type III: clinical and ultrastructural characteristics and distinction within the heterogeneous ichthyosis congenita group. Arch Dermatol Res 1988;280: 268-78.
207. Brusasco A, Gelmetti C, Tadini G, Caputo R. Ichthyosis congenita type IV: a new case resembling diffuse cutaneous mastocytosis. Br J Dermatol 1997;136:377-9.
208. Niemi KM, Kanerva L, Kuokkanen K. Recessive ichthyosis congenita type II. Arch Dermatol Res 1991;283:211-8.
209. Niemi KM, Kuokkanen K, Kanerva L, Ignatius J. Recessive ichthyosis congenita type IV. Am J Dermatopathol 1993;15: 224-8.
210. Niemi KM, Kanerva L, Kuokkanen K, Ignatius J. Clinical, light and electron microscopic features of recessive congenital ichthyosis type I. Br J Dermatol 1994;130:626-33.
211. Pigg M, Gedde-Dahl T Jr, Cox D, Hausser I, Anton-Lamprecht I, Dahl N. Strong founder effect for a transglutaminase 1 gene mutation in lamellar ichthyosis and congenital ichthyosiform erythroderma from Norway. Eur J Hum Genet 1998;6:589-96.
212. Descargues P, Deraison C, Prost C, Fraitag S, Mazereeuw-Hautier J, D'Alessio M, et al. Corneodesmosomal cadherins

are preferential targets of stratum corneum trypsin- and chymotrypsin-like hyperactivity in Netherton syndrome. J Invest Dermatol 2006;126:1622-32.
213. Wells RS, Kerr CB. The histology of ichthyosis. J Invest Dermatol 1966;46:530-5.
214. Fleckman P, Brumbaugh S. Absence of the granular layer and keratohyalin define a morphologically distinct subset of individuals with ichthyosis vulgaris. Exp Dermatol 2002;11: 327-36.
215. Bergman R, Khamaysi Z, Sprecher E. A unique pattern of dyskeratosis characterizes epidermolytic hyperkeratosis and epidermolytic palmoplantar keratoderma. Am J Dermatopathol 2008;30:101-5.
216. Ross R, DiGiovanna JJ, Capaldi L, Argenyi Z, Fleckman P, Robinson-Bostom L. Histopathologic characterization of epidermolytic hyperkeratosis: a systematic review of histology from the national registry for ichthyosis and related skin disorders. J Am Acad Dermatol 2008;59:86-90.
217. Sperling LC, DiGiovanna JJ. Curly" wood and tiger tails: an explanation for light and dark banding with polarization in trichothiodystrophy. Arch Dermatol 2003;139:1189-92.
218. Tay CH. Ichthyosiform erythroderma, hair shaft abnormalities, and mental and growth retardation: a new recessive disorder. Arch Dermatol 1971;104:4-13.
219. Schlucker S, Liang C, Strehle KR, DiGiovanna JJ, Kraemer KH, Levin IW. Conformational differences in protein disulfide linkages between normal hair and hair from subjects with trichothiodystrophy: a quantitative analysis by Raman microspectroscopy. Biopolymers 2006;82:615-22.
220. Liang C, Morris A, Schlucker S, Imoto K, Price VH, Menefee E, et al. Structural and molecular hair abnormalities in trichothiodystrophy. J Invest Dermatol 2006;126:2210-6.
221. Gruber R, Janecke AR, Fauth C, Utermann G, Fritsch PO, Schmuth M. Filaggrin mutations p.R501X and c.2282del4 in ichthyosis vulgaris. Eur J Hum Genet 2007;15:179-84.
222. Bitoun E, Micheloni A, Lamant L, Bonnart C, Tartaglia-Polcini A, Cobbold C, et al. LEKTI proteolytic processing in human primary keratinocytes, tissue distribution and defective expression in Netherton syndrome. Hum Mol Genet 2003;12:2417-30.
223. Ong C, O'Toole EA, Ghali L, Malone M, Smith VV, Callard R, et al. LEKTI demonstrable by immunohistochemistry of the skin: a potential diagnostic skin test for Netherton syndrome. Br J Dermatol 2004;151:1253-7.
224. Raghunath M, Tontsidou L, Oji V, Aufenvenne K, Schurmeyer-Horst F, Jayakumar A, et al. SPINK5 and Netherton syndrome: novel mutations, demonstration of missing LEKTI, and differential expression of transglutaminases. J Invest Dermatol 2004;123:474-83.
225. Raghunath M, Hennies HC, Velten F, Wiebe V, Steinert PM, Reis A, et al. A novel in situ method for the detection of deficient transglutaminase activity in the skin. Arch Dermatol Res 1998;290:621-7.
226. Hohl D, Aeschlimann D, Huber M. In vitro and rapid in situ transglutaminase assays for congenital ichthyoses—a comparative study. J Invest Dermatol 1998;110:268-71.
227. Jeon S, Djian P, Green H. Inability of keratinocytes lacking their specific transglutaminase to form cross-linked envelopes: absence of envelopes as a simple diagnostic test for lamellar ichthyosis. Proc Natl Acad Sci U S A 1998;95: 687-90.
228. Has C, Seedorf U, Kannenberg F, Bruckner-Tuderman L, Folkers E, Folster-Holst R, et al. Gas chromatography-mass spectrometry and molecular genetic studies in families with the Conradi-Hünermann-Happle syndrome. J Invest Dermatol 2002;118:851-8.
229. Traupe H, Burgdorf WHC. Treatment of ichthyosis—there is always something you can do! In Memoriam: Wolfgang Küster. J Am Acad Dermatol 2007;57:542-7.
230. Shwayder T. Disorders of keratinization: diagnosis and management. Am J Clin Dermatol 2004;5:17-29.
231. Kuster W. Ichthyoses: suggestions for an improved therapy. Dtsch Arztebl 2006;103:1484-9.
232. Oji V, Traupe H. Ichthyosis: clinical manifestations and practical treatment options. Am J Clin Dermatol 2009;10:351-64.
233. Yamamura S, Kinoshita Y, Kitamura N, Kawai S, Kobayashi Y. Neonatal salicylate poisoning during the treatment of a collodion baby. Clin Pediatr 2002;41:451-2.
234. Moskowitz DG, Fowler AJ, Heyman MB, Cohen SP, Crumrine D, Elias PM, et al. Pathophysiologic basis for growth failure in children with ichthyosis: an evaluation of cutaneous ultrastructure, epidermal permeability barrier function, and energy expenditure. J Pediatr 2004;145:82-92.
235. Fowler AJ, Moskowitz DG, Wong A, Cohen SP, Williams ML, Heyman MB. Nutritional status and gastrointestinal structure and function in children with ichthyosis and growth failure. J Pediatr Gastroenterol Nutr 2004;38:164-9.

BJD
British Journal of Dermatology

Partially disturbed lamellar granule secretion in mild congenital ichthyosiform erythroderma with *ALOX12B* mutations

M. Akiyama, K. Sakai, T. Yanagi, N. Tabata,* M. Yamada† and H. Shimizu

Department of Dermatology, Hokkaido University Graduate School of Medicine, North 15 West 7, Kita-ku, Sapporo 060-8638, Japan
**Division of Dermatology and †Department of Pediatrics and Neonatal Intensive Care Unit, Japanese Red Cross Sendai Hospital, Sendai, Japan*

Correspondence
Masashi Akiyama.
E-mail: akiyama@med.hokudai.ac.jp

Accepted for publication
17 February 2010

Key words
ichthyosis, keratinization, lipid, lipoxygenase, LOX

Conflicts of interest
None declared.

DOI 10.1111/j.1365-2133.2010.09745.x

Congenital ichthyosiform erythroderma (CIE) (OMIM 242100) is a major type of autosomal recessive congenital ichthyosis (ARCI) showing generalized scaling and erythroderma without blister formation.[1] Mutations in *ALOX12B* (OMIM 603741), encoding 12R-lipoxygenase (LOX), were identified in patients with CIE in 2002.[2] To date, several *ALOX12B* mutations have been reported in CIE families.[3,4] LOXs are a family of nonhaem, iron-containing dioxygenases which catalyse dioxygenation of fatty acids with one or more (Z,Z)-1,4-pentadiene moieties.[5] Three members of the human LOX family, 15-LOX-2, 12R-LOX and eLOX-3, are preferentially expressed in the skin.[5,6] The 12R-LOX pathway leads to hepoxilin B3 and trioxilin B3[7] resulting in 20-carboxy-trioxilin A3,[5] which is thought to be a key biological regulator in the skin.[8] 12R-LOX deficiency results in a CIE phenotype in humans[2,9,10] and in mice.[11,12] We report that a Japanese patient with CIE, harbouring one previously unreported *ALOX12B* mutation p.Arg442Gln and another known mutation p.Arg432X, showed partially disturbed secretion of lamellar granule (LG) contents in the epidermis.

Case and methods

The patient was the first child of healthy, unrelated Japanese parents. There was no family history of any related disorders. The male child was born via uncomplicated, vaginal full-term delivery. The newborn was covered by a collodion membrane and showed thick scales on a background of erythroderma over his entire body, with skin fissures on the trunk (Fig. 1a–c). Moderate ectropion and eclabium were seen. Hands and feet were oedematous, and the palms and soles were involved. The patient was treated with a topical application of white petrolatum with an occlusive dressing technique in a humid incubator. The hyperkeratosis and oedema were remarkably reduced within 2 weeks. At age 3·5 months, the patient showed mild white to grey-coloured scales over the erythematous skin covering his entire body (Fig. 1d–f).

Mutation analysis of *ALOX12B* was performed using genomic DNA isolated from peripheral blood cells of the patient and his parents.

Results and discussion

Mutation analysis of *ALOX12B* revealed that the patient was a compound heterozygote for a known nonsense mutation p.Arg432X (c.1294C>T) in exon 10 and a previously unreported missense mutation p.Arg442Gln (c.1325C>T) in exon 10 (GenBank NM_001139.2) (Fig. 1g, h). The nonsense mutation p.Arg432X was present in a heterozygous fashion in his mother, although p.Arg442Gln was not found in the parents and was thought to be a *de novo* mutation. The mutations were verified by mutant allele-specific amplification analysis. No mutation was found in the sequence analysis of 200 alleles from 100 normal, unrelated Japanese individuals, and therefore it is unlikely to be a polymorphism (data not shown). No other pathogenic mutations were found in *TGM1* (OMIM 190195), *ABCA12* (OMIM 607800), *NIPAL4* (ichthyin; OMIM 609383), *CYP4F22* (previously known as *FLJ39501*; OMIM 611495) or *ALOXE3* (OMIM 607206) by direct sequencing analysis.

p.Arg432X results in a serious truncation of the 12R-LOX peptide, losing approximately half of the C-terminal catalytic LOX domain, and is thought to have a serious effect on the enzyme activity.

The arginine residue mutated by p.Arg442Gln is in the central part of the C-terminal catalytic LOX domain and is highly conserved among diverse species (Fig. 1i) and human LOX family members (Fig. 1i). These facts suggest that this arginine residue might be essential for enzyme activity and that the present missense mutation affects 12R-LOX activity.

Electron microscopy of a skin biopsy specimen from the trunk at age 6 days using ruthenium tetroxide postfixation revealed irregular-sized lipid droplets in the stratum corneum.

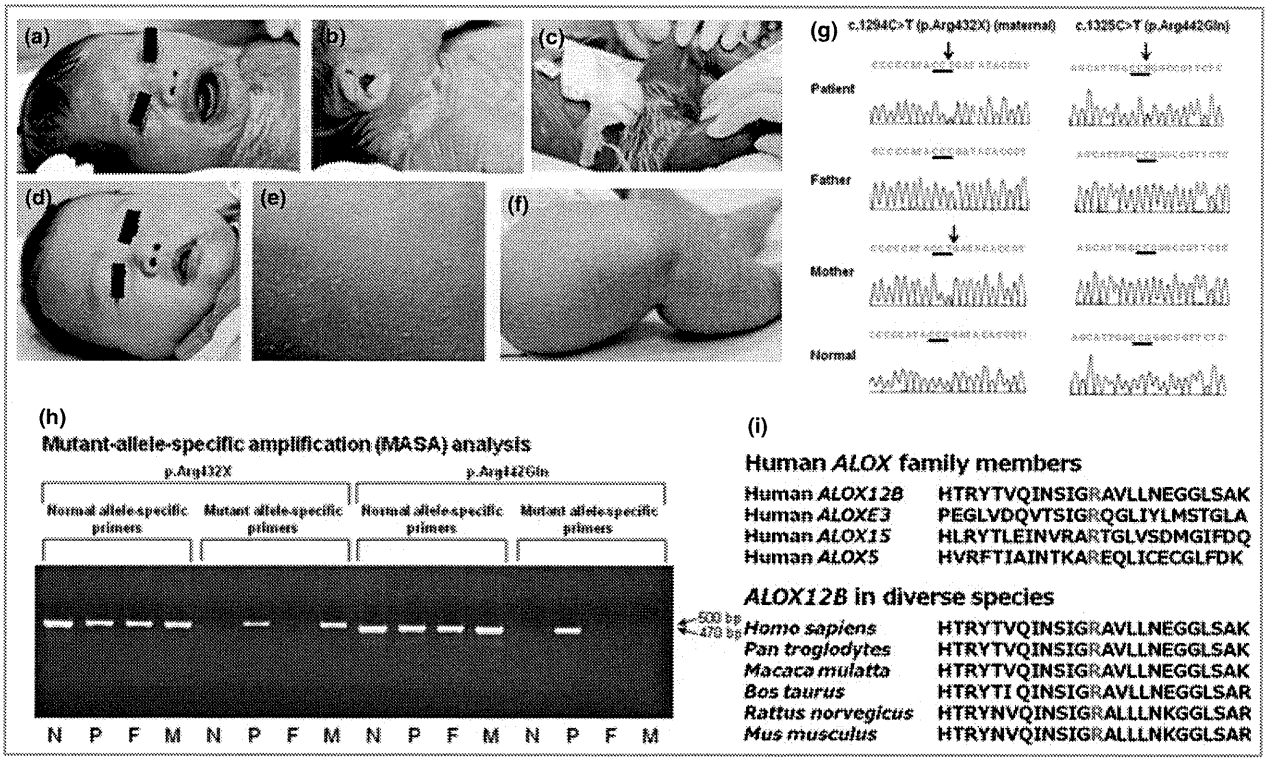

Fig 1. The patient's clinical features and compound heterozygous mutations in *ALOX12B*. (a–c) At 1 day of age: moderate ectropion and eclabium (a), a malformed auricle (b), and thick plate-like scales and fissures on the neck and the chest (b) and on the lower abdomen to the thigh (c). (d–f) At age 3·5 months: only slight, fine scales on the face (d), the back (e) and the thigh (f). (g) Compound heterozygous *ALOX12B* mutations, maternal p.Arg432X (c.1294C>T) and a novel missense mutation p.Arg442Gln (c.1325C>T) in exon 10 of the patient's genomic DNA. (h) Mutant allele-specific amplification (MASA) analysis showed a 500-bp band from p.Arg432X and a 470-bp band from p.Arg442Gln. N, normal; P, patient; F, father; M, mother. (i) Arginine 442 in 12*R*-lipoxygenase (LOX) altered by p.Arg442Gln; red character (R) is conserved among human *ALOX* family members (top) and diverse species (bottom).

Intact LGs were observed and intercellular lipid lamellae were seen in the intercellular space in the stratum corneum, although secretion of LG contents was disturbed in part in the granular layer cells (Fig. 2a–e).

Immunofluorescence staining revealed that one of the major basal keratins (keratin 5), differentiation-specific keratin (keratin 10) and ABCA12 were distributed normally in the basal layer, in the suprabasal layers, and in the granular layers, respectively, of the patient's epidermis (Fig. 2f, h, j). Immunoreactivity for cornified cell envelope-associated proteins involucrin, loricrin and transglutaminase 1 was seen normally distributed in the patient's upper epidermis (Fig. 2l, n, p).

Keratinocyte differentiation (keratinization)-specific molecules examined in the present study were normally distributed in the patient's epidermis. Also, keratinocyte differentiation defects were not morphologically or biochemically detected in *Alox12b*-disrupted mice.[11] These facts suggest that keratinocyte differentiation defects might not be involved in the pathogenesis of ichthyosis in CIE with *ALOX12B* mutations.

One report on ultrastructural features of the 12R-LOX-deficient human epidermis demonstrated lipid droplets in the cornified layers.[13] From the study of *Alox12b* mutant mouse skin transplants, it was suggested that 12R-LOX deficiency might affect the processing of LGs.[14] In *Alox12b*-disrupted mouse skin, irregular-sized vesicles were observed in the granular layers, and the stacks of lipid lamellae representing extruded content of LGs were seen in the transition zone between the uppermost granular and the first cornified cells.[11] In the present study, we clearly demonstrated lipid droplets in the cornified cell layers, and partially disturbed LG content secretion into the intercellular space in the patient's epidermis. Our results suggest that partially disturbed secretion of LG contents is involved in the pathogenesis of ichthyosis in patients with CIE with *ALOX12B* mutations. It has not been clarified completely yet how the partially disturbed secretion of LG contents contributes to the pathogenesis of CIE. Several ichthyosiform disorders have been shown to involve the abnormal function of LG.[1,15] Lipid contents secreted from LG are known to form the intercellular lipid layers in the stratum corneum.[16] The intercellular lipid layers are essential for the epidermal barrier function and the defective intercellular lipid layers caused by disturbed secretion of LG lipid contents are expected to result in skin barrier impairment.[17] Defective skin barrier function leads to compensatory mechanisms involving epidermal hyperproliferation and hyperkeratosis, which are

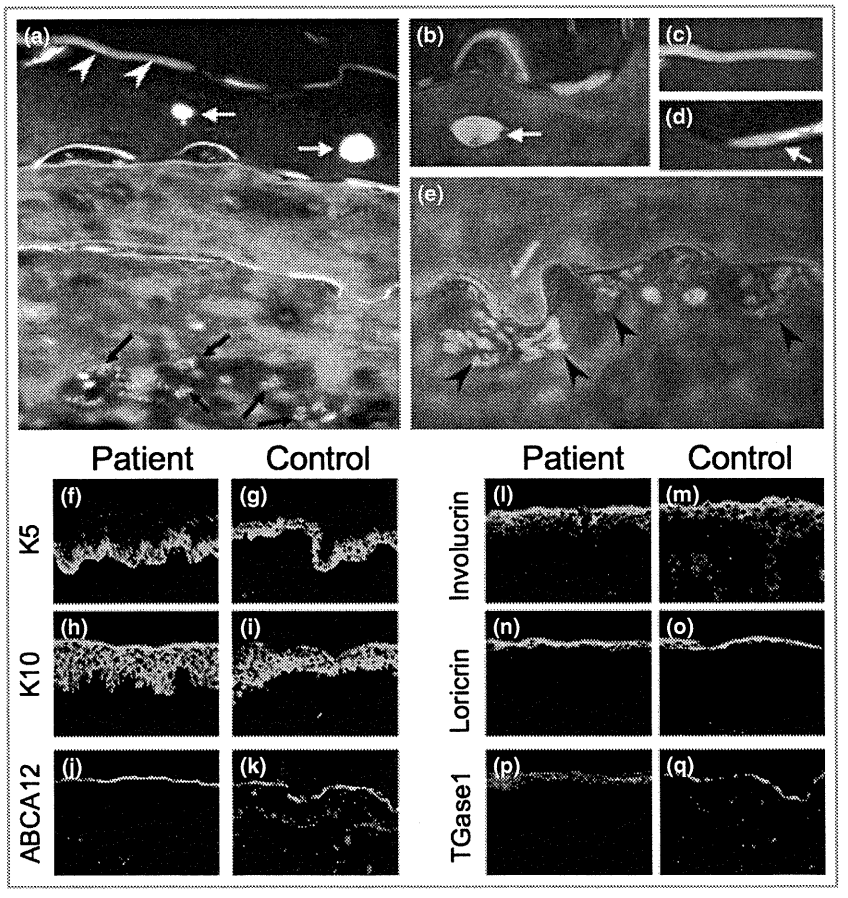

Fig 2. Disturbed secretion of lamellar granule (LG) contents from the granular layer cells and normal distribution of keratinization markers in the patient's epidermis. (a–e) Ultrastructural features of the skin biopsy specimen in the neonatal period. (a) Overall keratinization processes appeared normal. Black arrows, LGs; white arrowheads, intercellular lipid lamellae; white arrows, various-sized cytoplasmic lipid vacuoles. (b) An irregular-sized lipid vacuole (white arrow) containing the lamellar structure. (c) Intact intercellular lipid lamellae. (d) Normal cornified cell envelope (white arrow). (e) Partially congested LG secretion (arrowheads) in a granular layer cell. (f–q) Immunofluorescence staining (FITC) revealed that keratin 5, keratin 10 and ABCA12 were distributed normally in the basal layer, suprabasal layers and granular layers, respectively. For keratin 5 immunostaining, we used an antibody which cross-reacts with keratin 8. However, the labelling of this antibody is thought to reflect keratin 5 expression in this study, because keratin 8 expression is usually restricted to the simple epithelia. Cornified cell envelope-associated proteins, involucrin, loricrin and transglutaminase 1, were seen normally distributed in the upper epidermis. (f–q) Nuclear stain, red (propidium iodide). Original magnification: (a) × 6000, (b) × 12 000, (c, d) × 18 000, (e) × 10 000, (f–q) × 20.

observed frequently in ichthyosiform diseases.[16] In this context, we can hypothesize that the partially disturbed secretion of LG contents might cause defective intercellular lipid layers in the stratum corneum, resulting in skin barrier defects and subsequent compensatory hyperkeratosis in CIE.

Patients with CIE harbouring *ALOX12B* mutations have previously been reported in African and European populations.[3,4] Our previous studies failed to identify *ALOX12B* mutations in Japanese patients with ARCI[18] and demonstrated that the frequency of *ALOX12B* mutations is expected to be low in Japanese patients with ARCI. As far as we know, the present case is the first patient with CIE with detected *ALOX12B* mutations in the Asian area and our results also confirm *ALOX12B* as one of the CIE causative genes in the Asian population. Further accumulation of CIE cases is needed to clarify the frequency of *ALOX12B* mutations in patients with CIE in Asian countries.

Acknowledgments

We thank Dr James R. McMillan for proofreading this manuscript and Ms Yuki Miyamura for her fine technical assistance on this project. This work was supported in part by a Grant-in-Aid from the Ministry of Education, Science, Sports and Culture of Japan to M.A. (Kiban B 20390304) and by a grant from the Ministry of Health, Labor and Welfare of Japan (Health and Labor Sciences Research Grants; Research on Intractable Diseases; H21-047) to M.A.

References

1 Akiyama M, Shimizu H. An update on molecular aspects of the non-syndromic ichthyoses. *Exp Dermatol* 2008; **42**:83–9.
2 Jobard F, Lefèvre C, Karaduman A *et al.* Lipoxygenase-3 (*ALOXE3*) and 12(R)-lipoxygenase (*ALOX12B*) are mutated in non-bullous

congenital ichthyosiform erythroderma (NCIE) linked to chromosome 17p13.1. *Hum Mol Genet* 2002; **11**:107–13.

3 Eckl KM, de Juanes S, Kurtenbach J *et al.* Molecular analysis of 250 patients with autosomal recessive congenital ichthyosis: evidence for mutation hotspots in *ALOXE3* and allelic heterogeneity in *ALOX12B*. *J Invest Dermatol* 2009; **129**:1421–8.

4 Fischer J. Autosomal recessive congenital ichthyosis. *J Invest Dermatol* 2009; **129**:1319–21.

5 Brash AR, Yu Z, Boeglin WE, Schneider C. The hepoxilin connection in the epidermis. *FEBS J* 2007; **274**:3494–502.

6 Krieg P, Heidt M, Siebert M *et al.* Epidermis-type lipoxygenases. *Adv Exp Med Biol* 2002; **507**:165–70.

7 Anton R, Camacho M, Puig L, Vila L. Hepoxilin B3 and its enzymatically formed derivative trioxilin B3 are incorporated into phospholipids in psoriatic lesions. *J Invest Dermatol* 2002; **118**:139–46.

8 Lefèvre C, Bouadjar B, Ferrand V *et al.* Mutations in a new cytochrome P450 gene in lamellar ichthyosis type 3. *Hum Mol Genet* 2006; **15**:767–76.

9 Eckl KM, Krieg P, Küster W *et al.* Mutation spectrum and functional analysis of epidermis-type lipoxygenases in patients with autosomal recessive congenital ichthyosis. *Hum Mutat* 2005; **26**:351–61.

10 Yu Z, Schneider C, Boeglin WE, Brash AR. Mutations associated with a congenital form of ichthyosis (NCIE) inactivate the epidermal lipoxygenases 12R-LOX and eLOX3. *Biochim Biophys Acta* 2005; **3**:238–47.

11 Epp N, Fürstenberger G, Müller K *et al.* 12R-lipoxygenase deficiency disrupts epidermal barrier function. *J Cell Biol* 2007; **177**:173–82.

12 Moran J, Qiu H, Turbe-Doan A *et al.* A mouse mutation in the 12R-lipoxygenase, *Alox12b*, disrupts formation of the epidermal permeability barrier. *J Invest Dermatol* 2007; **127**:1893–7.

13 Harting M, Brunetti-Pierri N, Chan CS *et al.* Self-healing collodion membrane and mild nonbullous congenital ichthyosiform erythroderma due to 2 novel mutations in the *ALOX12B* gene. *Arch Dermatol* 2008; **144**:351–6.

14 de Juanes S, Epp N, Latzko S *et al.* Development of an ichthyosiform phenotype in *Alox12b*-deficient mouse skin transplants. *J Invest Dermatol* 2009; **129**:1429–36.

15 Hershkovitz D, Mandel H, Ishida-Yamamoto A *et al.* Defective lamellar granule secretion in arthrogryposis, renal dysfunction, and cholestasis syndrome caused by a mutation in *VPS33B*. *Arch Dermatol* 2008; **144**:334–40.

16 Elias PM. Stratum corneum defensive functions: an integrated view. *J Invest Dermatol* 2005; **125**:183–200.

17 Yanagi T, Akiyama M, Nishihara H *et al.* Harlequin ichthyosis model mouse reveals alveolar collapse and severe fetal skin barrier defects. *Hum Mol Genet* 2008; **17**:3075–83.

18 Sakai K, Akiyama M, Yanagi T *et al.* *ABCA12* is a major causative gene for non-bullous congenital ichthyosiform erythroderma. *J Invest Dermatol* 2009; **129**:2306–9.

RESEARCH ARTICLE

Human Mutation

OFFICIAL JOURNAL
HGVS
HUMAN GENOME VARIATION SOCIETY
www.hgvs.org

Prevalent *LIPH* Founder Mutations Lead to Loss of P2Y5 Activation Ability of PA-PLA$_1\alpha$ in Autosomal Recessive Hypotrichosis

Satoru Shinkuma,[1] Masashi Akiyama,[1]* Asuka Inoue,[2] Junken Aoki,[2] Ken Natsuga,[1] Toshifumi Nomura,[1,3] Ken Arita,[1] Riichiro Abe,[1] Kei Ito,[1] Hideki Nakamura,[1] Hideyuki Ujiie,[1] Akihiko Shibaki,[1] Hiraku Suga,[4] Yuichiro Tsunemi,[4] Wataru Nishie,[1] and Hiroshi Shimizu[1]

[1]Department of Dermatology, Hokkaido University Graduate School of Medicine, Sapporo 060-8638, Japan; [2]Graduate School of Pharmaceutical Sciences, Tohoku University, Sendai 980-8578, Japan; [3]Epithelial Genetics Group, Division of Molecular Medicine, Colleges of Life Science and Medicine, Dentistry & Nursing, University of Dundee, Dundee, DD1 5EH, United Kingdom; [4]Department of Dermatology, Tokyo University, Faculty of Medicine 113-8655, Tokyo, Japan

Communicated by David S. Rosenblatt

Received 8 January 2010; accepted revised manuscript 22 February 2010.
Published online 8 March 2010 in Wiley InterScience (www.interscience.wiley.com). DOI 10.1002/humu.21235

ABSTRACT: Autosomal recessive hypotrichosis (ARH) is characterized by sparse hair on the scalp without other abnormalities. Three genes, *DSG4*, *LIPH*, and *LPAR6* (*P2RY5*), have been reported to underlie ARH. We performed a mutation search for the three candidate genes in five independent Japanese ARH families and identified two *LIPH* mutations: c.736T>A (p.Cys246Ser) in all five families, and c.742C>A (p.His248Asn) in four of the five families. Out of 200 unrelated control alleles, we detected c.736T>A in three alleles and c.742C>A in one allele. Haplotype analysis revealed each of the two mutant alleles is derived from a respective founder. These results suggest the *LIPH* mutations are prevalent founder mutations for ARH in the Japanese population. *LIPH* encodes PA-PLA$_1\alpha$ (LIPH), a membrane-associated phosphatidic acid-preferring phospholipase A$_1\alpha$. Two residues, altered by these mutations, are conserved among PA-PLA$_1\alpha$ of diverse species. Cys^{246} forms intramolecular disulfide bonds on the lid domain, a crucial structure for substrate recognition, and His^{248} is one amino acid of the catalytic triad. Both p.Cys246Ser- and p.His248Asn-PA-PLA$_1\alpha$ mutants showed complete abolition of hydrolytic activity and had no P2Y5 activation ability. These results suggest defective activation of P2Y5 due to reduced 2-acyl lysophosphatidic acid production by the mutant PA-PLA$_1\alpha$ is involved in the pathogenesis of ARH.
Hum Mutat 31:602–610, 2010. © 2010 Wiley-Liss, Inc.

KEY WORDS: LIPH; Lysophosphatidic Acid; Phosphatidic Acid; Lid Domain; Catalytic Triad; LAH2; LAH

Introduction

Autosomal recessive hypotrichosis (ARH; MIM#s 607892, 607903, 611452) is a rare form of alopecia characterized by sparse hair on the scalp, sparse to absent eyebrows and eyelashes, and sparse axillary and body hair. Wali et al. [2007] noted clinical similarities among three genetically distinct forms of hypotrichosis, localized autosomal recessive hypotrichosis (LAH), and proposed that the forms mapped to chromosome 18q12.1, 3q27.2, and 13q14.11–q21.32 are designated as LAH1, LAH2, and LAH3, respectively. Recently, causative genes for all three forms were identified. Mutations in the desmoglein-4 gene (*DSG4*; MIM# 607892) lead to LAH1 [Kljuic et al., 2003; Rafique et al., 2003]. Mutations in *LIPH* (MIM# 607365), which encodes membrane-associated phosphatidic acid-preferring phospholipase A$_1\alpha$ (PA-PLA$_1\alpha$[LIPH]), underlie LAH2 [Ali et al., 2007; Kazantseva et al., 2006]. Most recently, Pasternack et al. [2008] and Shimomura et al. [2008] reported that mutations in the lysophosphatidic acid receptor 6 gene *LPAR6* (*P2RY5*; MIM# 609239) caused LAH3.

In this study, we searched for mutations in the *DSG4*, *LIPH*, and *LPAR6* genes in five unrelated Japanese families with ARH. Surprisingly, we found two prevalent missense mutations in the *LIPH* gene in all of the families. Furthermore, one mutation c.736T>A (p.Cys246Ser) was found in all five families, and the other mutation c.742C>A (p.His248Asn) was detected in four of the five families. We clarified that these two mutations are strong founder mutations in *LIPH* in the Japanese population. In addition, we evaluated the enzyme activity of mutant PA-PLA$_1\alpha$ derived from the two mutant alleles. We also analyzed the abilities of the mutant PA-PLA$_1\alpha$ to activate lysophosphatidic acid receptor 6 (P2Y5), to clarify the pathogenetic pathway of ARH.

Materials and Methods

Subjects

Five unrelated nonconsanguineous Japanese families A, B, C, D, and E (Fig. 1) with ARH were seen in our hospital or referred to us for the past 5 years. Families A, C, and D were from Hokkaido, the northern most major island of Japan. Families B and E were from western and central Japan, respectively. The medical ethics committee of Hokkaido University approved all the described studies. The study was conducted according to the Declaration of Helsinki Principles. The patients gave written informed consent.

*Correspondence to: Masashi Akiyama, Department of Dermatology, Hokkaido University Graduate School of Medicine, North 15 West 7, Sapporo 060-8638, Japan. E-mail: akiyama@med.hokudai.ac.jp

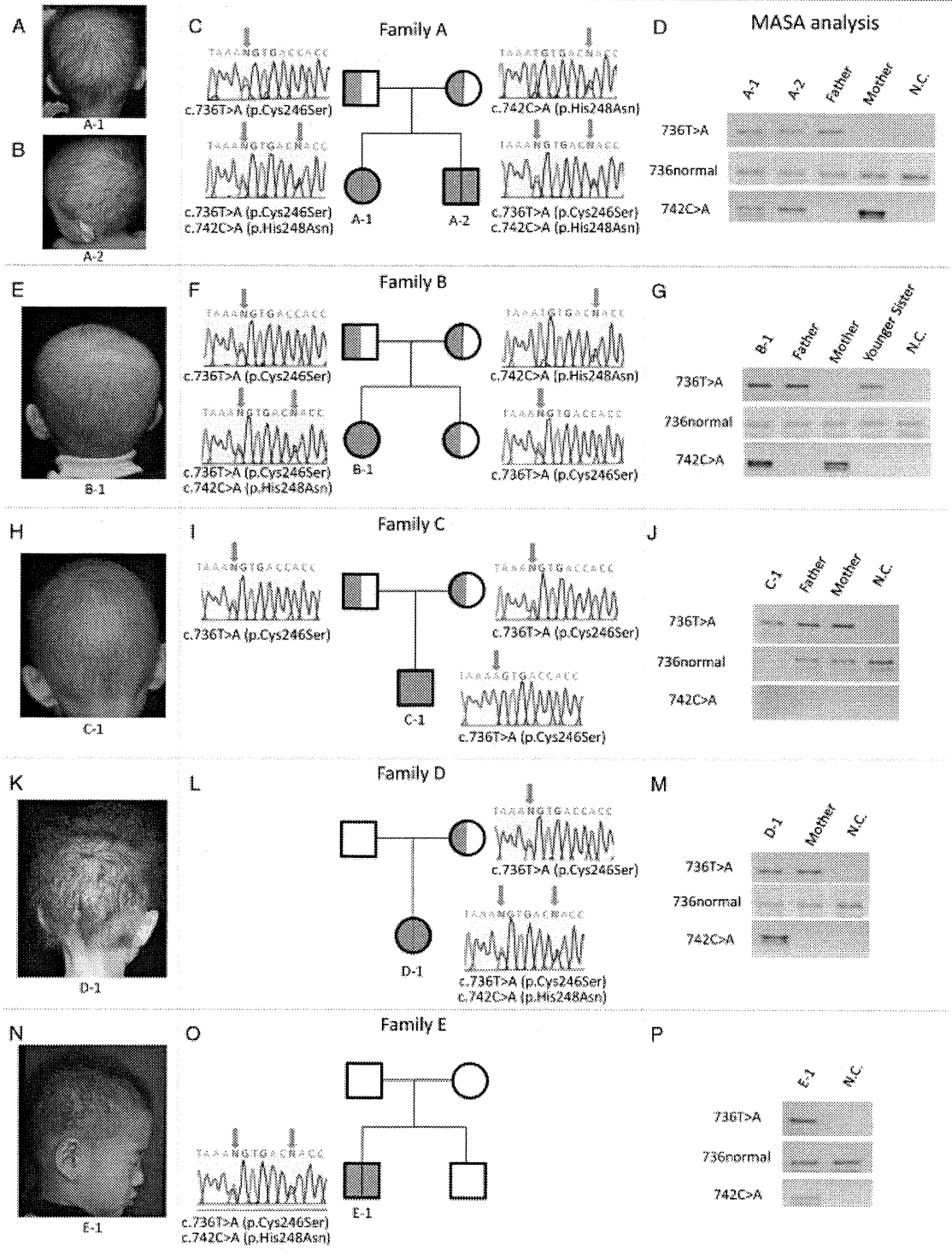

Figure 1. Clinical features of five Japanese families with ARH and identification of mutations in the *LIPH* gene. **A, B, E, H, K, N:** All the affected individuals have features of ARH, which is characterized by sparse hair on the scalp and slightly sparse to absent eyebrows and eyelashes. **C, F, I, L, O:** Pedigrees of the families. Family A (C), Family B (F), Family C (I), Family D (L), and Family E (O) are consistent with autosomal recessive inheritance. Direct sequencing of the *LIPH* gene revealed that patients A-1, A-2, B-1, D-1, and E-1 had compound heterozygous missense mutations involving c.736T>A and c.742C>A, whereas patient C-1 had a homozygous c.736T>A missense mutation. **D, G, J, M, P:** Mutant-allele-specific amplification (MASA) analysis. (Upper) With c.736T>A mutant allele-specific primers, the amplification bands from the c.736T>A mutant alleles are detected by direct sequencing as 301 bp fragments only in the patients and their family members who had the c.736T>A missense mutation, confirming the presence of the mutation. (Middle) With c.736 wild-type allele-specific primers, no PCR product was detected in patient C-1, who was homozygous for c.736T>A. PCR products from the other patients who were compound heterozygous for the two missense mutations c.736T>A and c.742C>A, from unaffected family members and from the normal control (N.C.) were amplified by wild-type allele-specific amplification. (Lower) With c.742C>A mutant-allele-specific primers, the amplification bands from the c.742C>A mutant alleles were detected as 297 bp fragments only in the PCR products from the DNA samples of the patients and their family members who had the c.742C>A missense mutation, confirming the presence of the mutation.

Mutation Detection

DSG4, *LIPH*, and *LPAR6* mutation search was performed as previously reported [Moss et al., 2004; Pasternack et al., 2008; Shimomura et al., 2008, 2009b]. Briefly, genomic DNA (gDNA) isolated from peripheral blood was subjected to polymerase chain reaction (PCR) amplification, followed by direct automated sequencing using an ABI PRISM 3100 genetic analyzer (Advanced Biotechnologies, Columbia, MD), and verification of the mutations by mutant-allele-specific amplification (MASA) analysis.

Oligonucleotide primers were designed using the Website program (www.bioinformatics.nl/cgi-bin/primer3plus/primer3plus.cgi). The entire coding regions of *DSG4*, *LIPH*, and *LPAR6*, including the exon/intron boundaries, were sequenced using gDNA samples from patients and their family members, after fully informed consent. For normal controls, 100 healthy unrelated Japanese individuals (200 normal alleles) were studied.

The complementary DNA (cDNA) nucleotides and the amino acids of the protein were numbered based on the previous sequence information (GenBank accession number, *DSG4*; AY177664.1, *LIPH*; AY093498.1, *LPAR6*; AF000546.1) [Jin et al., 2002; Whittock and Bower, 2003]. Nucleotide numbering reflects cDNA numbering with +1 corresponding to the A of the ATG translation initiation codon in the reference sequence, according to journal guidelines (www.hgvs.org/mutnomen). The initiation codon is codon 1.

Mutant Allele-Specific Amplification Analysis

For verification of the mutation, using PCR products as a template, mutant allele specific amplification analysis was performed with mutant allele-specific primers carrying the substitution of a base at the 3′-end [Hasegawa et al., 1995; Xu et al., 2003], as follows: c.736T>A mutant allele-specific forward primer, 5′-CCAAGGATTTCAGTATTTTAAAA-3′; c.736 normal allele-specific forward primer, 5′-CCAAGGATTTCAGTATTT-TAAAT-3′; c.742C>A mutant allele-specific forward primer, 5′-GGATTTCAGTATTTTAAATGTGACA-3′; reverse primer, 5′-GTGCCCAGCAGAAAAACAAG-3′.

PCR conditions were as follows: 94°C for 5 min, followed by 35 cycles at 94°C for 1 min, 60°C (for c.736T>A mutant amplification) or 64°C (for c.742C>A mutant amplification) for 1 min, and extension at 72°C for 7 min. Only 301- and 297-bp fragments derived from the mutant alleles were amplified with these primers and the PCR condition, respectively.

Haplotype Analysis

To determine whether the mutations c.736T>A and c.742C>A are founder mutations, we performed haplotype analysis. We constructed linkage disequilibrium (LD) blocks containing the *LIPH* gene using genotype data from the HapMap database (International HapMap Consortium, 2005). The haplotype structure with its tag-single nuclotide polymorphisms (SNPs) was determined using Haploview [Barrett et al., 2005]. We genotyped 10 tag-SNPs using the ABI PRISM 3100 genetic analyzer (Advanced Biotechnologies). Oligonucleotide primers were designed using the website program (www.bioinformatics.nl/cgi-bin/primer3plus/primer3plus.cgi).

Construction of Mutated *LIPH* Gene Expression Vectors

Normal human full-length *LIPH* cDNA was amplified by reverse transcription-PCR using human colon-derived total RNA [Sonoda et al., 2002]. The DNA fragment covering the coding region of PA-PLA$_1\alpha$ (EcoRI–EcoRI fragment) was subcloned into the EcoRI site of pCAGGS mammalian expression vector (kindly donated by Dr. Junichi Miyazaki, Osaka University) [Hiramatsu et al., 2003]. Short *LIPH* fragments (64 bp) (c.695–758) including either the c.736T>A or the c.742C>A mutation were synthesized by IDT Inc. (Coralville, IA). pCAGGS vector including the rest of the *LIPH* gene was amplified with specific primers as follows: forward (5′-CCTGTACCTGTCTTCCCTGAG-3′) and reverse (5′-CAGGTTGATCCAATCCTCCA-3′). PCR was carried out using KOD-Plus-Ver.2 (Toyobo, Osaka, Japan) according to the instructions. Finally, the synthesized mutated DNA fragments were ligated with the amplified pCAGGS vector including the *LIPH* gene without 64 bp oligonucleotide (c.695–758) using a Ligation-Convenience Kit (Nippon Gene Co., Tokyo, Japan).

Expression of Mutated PA-PLA$_1\alpha$ in HEK293 Cells

To investigate the molecular defects underlying the mutations that were identified in this study, we synthesized p.Cys246Ser or p.His248Asn mutations in PA-PLA$_1\alpha$ expression constructs and compared mutant protein expression with wild-type (WT) and p.Ser154Ala PA-PLA$_1\alpha$ protein. Previously, Sonoda et al. [2002] reported that Ser^{154} was the active catalytic residue and that the p.Ser154Ala mutant PA-PLA$_1\alpha$ had complete loss of enzyme activity, although the amount of p.Ser154Ala mutant protein expressed was almost the same as that of WT protein. Thus, we used the p.Ser154Ala mutant as a loss-of-function mutant control in this study.

HEK293 cells were maintained in Dulbecco's modified Eagle's medium supplemented with antibiotics and 10% fetal bovine serum under an atmosphere of 5% CO_2 at 37°C. The resulting cDNAs were used to transfect HEK293 cells using LipofectAMINE 2000 reagent (Invitrogen, Carlsbad, CA) according to the manufacturer's protocol. HEK293 cells were transfected with WT, p.Ser154Ala (control loss-of-function mutant) [Sonoda et al., 2002], p.Cys246Ser or p.His248Asn PA-PLA$_1\alpha$.

Preparation of Cell Supernatants and Lysates and Western Blotting

HEK293 cells transfected with pCAGGS vector were maintained for an additional 24 hr after the medium was changed to serum-free medium ExCell302 (JRH Biosciences, Lenexa, KS). After 24 hr of incubation, the media were collected and precipitated with trichloroacetic acid. Precipitated protein was collected by centrifugation at 15,000 × *g* for 20 min, followed by washing with acetone twice; then, the pellet was redissolved in sodium dodecyl sulfate (SDS) sample buffer A (62.5 mM Tris-HCl [pH 6.8], 10% Glycerol, 2% SDS, 5% 2-mercaptoethanol (2ME), 10 μg/mL phenylmethylsulphonyl fluoride [PMSF]) and boiled for 5 min. HEK293 cells were harvested 48 hr after transfection and SDS sample buffer B (62.5 mM Tris-HCl [pH 6.8], 4 M Urea, 10% Glycerol, 2% SDS, 5% 2ME, 10 μg/mL PMSF) was added directly to the cell pellet. The pellet was then sonicated and boiled for 5 min.

These protein samples of cell supernatants and lysates were separated by SDS-polyacrylamide gel electrophoresis (SDS-PAGE) and transferred to nitrocellulose membrane. The nitrocellulose membrane was blocked with Tris-buffered saline containing 5% (w/v) skimmed milk and 0.05% (v/v) Tween 20, incubated with anti-PA-PLA$_1\alpha$ monoclonal antibody [Sonoda et al., 2002], and then treated with antirat IgG antibody conjugated with horseradish peroxidase. Proteins bound to the antibodies were

visualized with an enhanced chemiluminescence kit (ECL, Amersham Biosciences, Piscataway, NJ) by LAS4000 Luminescent Image Analyzer (Fujifilm, Tokyo, Japan) [Sonoda et al., 2002].

PA-PLA$_1\alpha$ Enzyme Activity Assay

PA-PLA$_1\alpha$ produces 2-acyl lysophosphatidic acid (LPA) and free fatty acid (FFA) concurrently from phosphatidic acid (PA) [Sonoda et al., 2002]. In the present study, the hydrolysis activity was determined measuring oleic acids, which are concurrently produced from dioleoyl PA by PA-PLA$_1\alpha$. We added the supernatant from HEK293 cells transfected with WT, p.Ser154Ala, p.Cys246Ser, or p.His248Asn PA-PLA$_1\alpha$ to the medium including 100 μM PA. After 12 hr incubation at 37°C, the amount of oleic acids was measured with NEFA C-Test Wako test kit (Wako Chemicals Co., Osaka, Japan).

P2Y5 Activation Ability Assay

We cotransfected alkaline-phosphatase-tagged transforming growth factor-α (AP-TGFα) (kindly provided by Dr. Higashiyama, Ehime University, Japan) [Tokumaru et al., 2000], recombinant P2Y5 and WT, p.Ser154Ala, p.Cys246Ser, or p.His248Asn PA-PLA$_1\alpha$ to HEK293 cells, and we quantified free AP-TGFα induced by a disintegrin and metalloprotease (ADAM) in the HEK293 cells to examine the P2Y5 activation ability of LPA produced by mutant PA-PLA$_1\alpha$. Cells were cultured in 100 μL of serum-free medium Opti-MEM (Gibco BRL, Grand Island, NY) in individual wells of a 96-well plate. After 24 hr of incubation, 80 μL of the conditioned medium in each well was transferred and AP activities in both the conditioned media and the transfected cells were measured using *p*-nitrophenyl phosphate (*p*-NPP). In the case of phorbol ester, 12-O-tetradecanoylphorbol-13-acetate (TPA)-stimulation, the transfected cells were treated with 100 nM 1 h before medium transfer. The AP reaction was performed in *p*-NPP buffer (5 mM *p*-NPP, 20 mM Tris-HCl (pH 9.5), 20 mM NaCl, and 5 mM $MgCl_2$) at 37°C for 1 hr and the increases in the reaction product, *p*-nitrophenol, were quantified by monitoring absorbance at 405 nm with VersaMax microplate reader (Molecular Devices, Sunnyvale, CA). The amount of AP-TGFα released was expressed as a ratio of AP activity in the conditioned media to total AP activity in each well.

Results

Clinical Findings

All six affected individuals in the five unrelated Japanese families showed features typical of ARH (Fig. 1A, B, E, H, K, and N). The patients were less than 10 years of age at the time of the study. Affected individuals had tightly curled hair, which grew slowly and stopped growing after a few inches. Their eyebrows and eyelashes were a little sparse to absent. Nails, teeth, sweating, and hearing were normal in all the affected individuals. Heterozygous carriers had normal hair. The pedigrees of all the families were consistent with autosomal recessive inheritance (Fig. 1C, F, I, L, and O).

Mutation Detection

Direct sequencing analysis of exons and intron–exon boundaries of *LIPH* revealed that affected members of Families A, B, D, and E were compound heterozygous for the two missense mutations c.736T>A (p.Cys246Ser) and c.742C>A (p.His248Asn) (Fig. 1C, F, I, L, O). The affected individual in Family C was homozygous for c.736T>A. All the parents whose DNA was available for mutation search were heterozygous carriers of one of the two mutations (Fig. 1C, F, I, L, and O). We confirmed these *LIPH* mutations by MASA analysis (Fig. 1D, G, J, M, and P). Both amino acid residues altered by the two missense mutations were highly conserved among diverse species (Fig. 2A). One of the mutations was found in 4/200 normal unrelated alleles (100 healthy Japanese individuals) by direct sequence analysis (minor allele frequency, c.736T>A, 0.015 (3/200); c. 742C>A, 0.005 (1/200); combined genotype 0.02 (4/200)), although there was no control individual who had compound heterozygous or homozygous mutations (data not shown). No other pathogenic mutation was found in the entire exon or intron/exon borders of the *DSG4*, *LIPH* or *LPAR6* gene.

Haplotype Aanalysis

The haplotype block structure containing the *LIPH* gene was constructed using genotype data from the HapMap database (Fig. 3B). The haplotype block was represented by five haplotypes with >1% frequency (Fig. 3C). The haplotype of the chromosome containing the *LIPH* c.736T>A mutation was found to have resulted from parent-to-child transmission in all five families (Table 1). The chromosome containing the *LIPH* c.736T>A mutation had haplotype I (ATCAACCGGA), which is seen in 37.8% of the Han Chinese and ethnic Japanese populations. Likewise, we determined the haplotype of the chromosome containing the *LIPH* c.742C>A mutation in four families (A, B, D, E). The chromosome containing the *LIPH* c.742C>A mutation had haplotype III (GCTCGTGAGG), which is seen in 28.9%. Thus, these missense mutations c.736T>A (p.Cys246Ser) and c.742C>A (p.His248Asn) in Japanese patients appear to represent founder effects in this island nation.

Expression of PA-PLA$_1\alpha$ in Mammalian Cells

Immunoblot analysis revealed that transfection of p.Cys246Ser and p.His248Asn mutant constructs into HEK293 cells resulted in the secretion of 55-kDa mutant PA-PLA$_1\alpha$ at a level similar to that of the WT and of the p.Ser154Ala mutant (Fig. 4A). In addition, the same amounts of mutant PA-PLA$_1\alpha$ proteins were also recovered from the cell lysate. These results indicated that there was no significant difference in protein yield between WT and mutant PA-PLA$_1\alpha$.

Analysis of PA-PLA$_1\alpha$ Hydrolytic Activity

The hydrolysis activity was determined measuring FFA which are concurrently produced from PA by PA-PLA$_1\alpha$. The quantities of FFA produced by the p.Cys246Ser and p.His248Asn mutant *LIPH* constructs were similar to those by the mock and p.Ser154Ala mutant constructs, suggesting that the p.Cys246Ser and p.His248Asn mutant PA-PLA$_1\alpha$ had no hydrolytic activity (Fig. 4B).

P2Y5 Activation Ability of PA-PLA$_1\alpha$ Mutants

In this study, we cotransfected AP-TGFα, recombinant P2Y5 and WT, p.Ser154Ala, p.Cys246Ser, or p.His248Asn PA-PLA$_1\alpha$ constructs to HEK293 cells. To examine the P2Y5 activation potency of mutant PA-PLA$_1\alpha$, AP-TGFα release into conditioned media via ADAM, which was triggered by activation of P2Y5, was

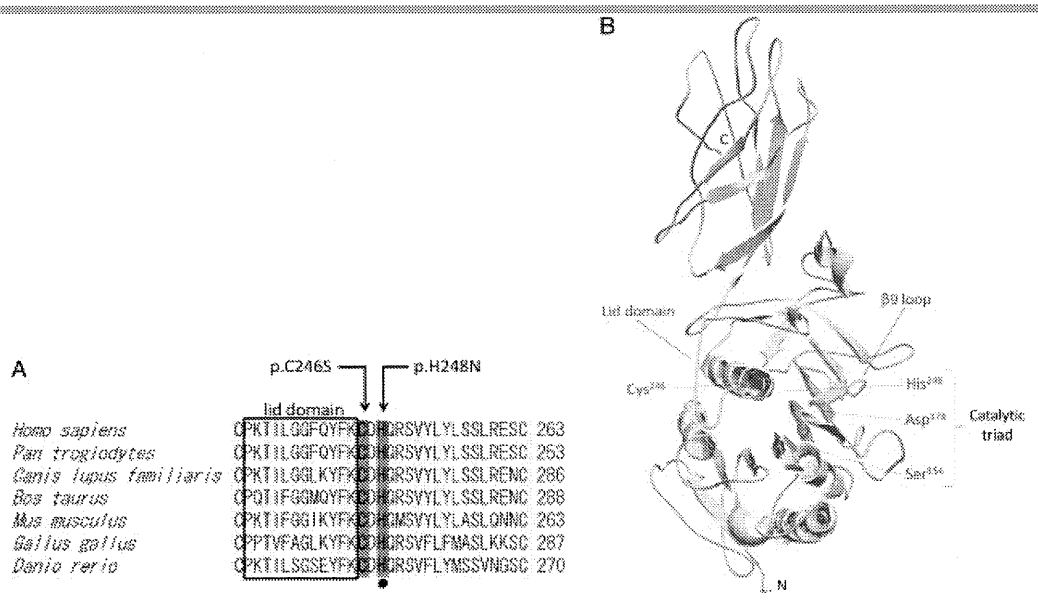

Figure 2. Conservation of the mutated residues and the three-dimensional protein structure around the mutation sites. **A**: Multiple amino acid sequence alignments of PA-PLA$_1\alpha$ of diverse species. Amino acid residues Cys^{246} and His^{248} altered by the present two mutations are highly conserved among PA-PLA$_1\alpha$ of diverse species. Amino acid residues that are conserved between the seven species are shown in yellow. The 12 residues that comprise the lid domain are surrounded by a black rectangle. One of the amino acids of the catalytic triad, His^{248}, is marked with a black dot. Cys^{246} and His^{248} are in red and indicated by arrows. **B**: The three-dimensional-structure model of PA-PLA$_1\alpha$ protein. Cys^{246} and His^{248} residues are in red. Lid domain and β9loop are in green. Catalytic triad consists of Ser^{154} (purple), Asp^{178} (purple) and His^{248}. Cys^{246} forms intramolecular disulfide bonds on the lid domain.

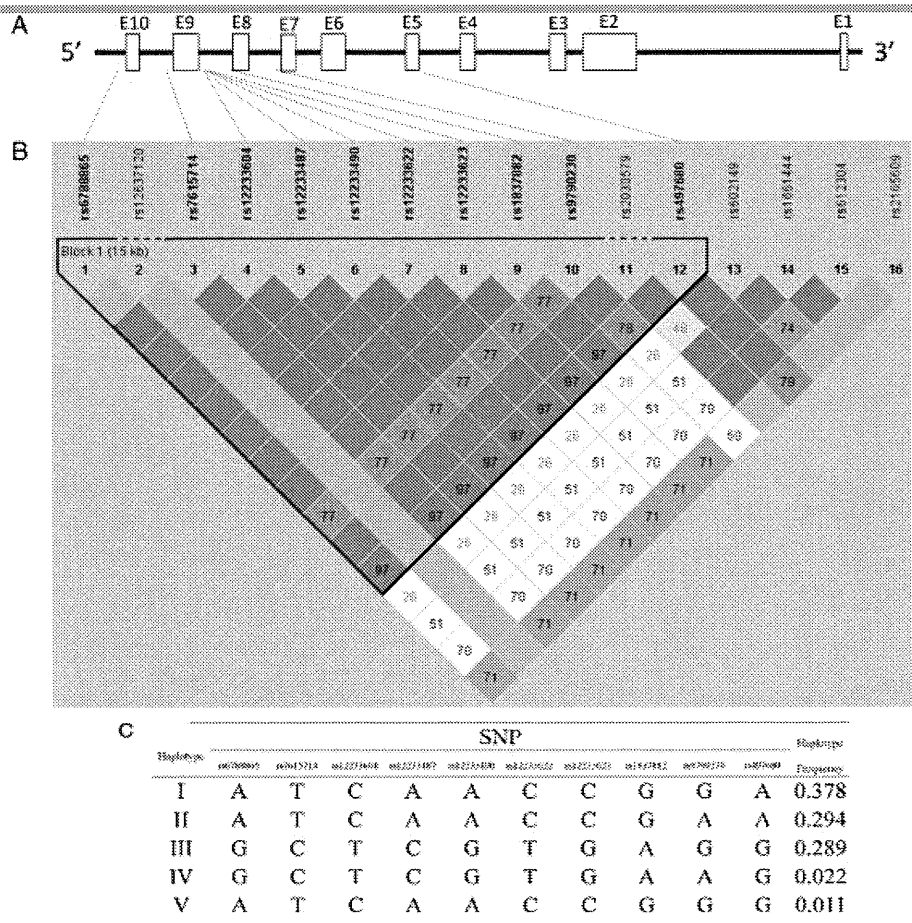

Figure 3. The linkage disequilibrium (LD) block and the haplotype structure around *LIPH* in Han Chinese and ethnic Japanese populations. *LIPH* structure (**A**) and the LD block within *LIPH* (**B**) were evaluated using genotype data from the HapMap database. **C**: The haplotype structure with 10 tag-SNPs was determined using Haploview.

Table 1. Identified Haplotype with the *LIPH* c.736T>A and c.742C>A Mutation

Family	Mutation	rs6788865	rs7615714	rs12233604	rs12233487	rs12233490	rs12233622	rs12233623	rs1837882	rs9790230	rs497680	Haplotype
A	c.736T>A	A/G	T/C	C/T	A/C	A/G	C/T	C/G	G/A	G/G	A/G	I/III
	c.742C>A	A/G	T/C	C/T	A/C	A/G	C/T	C/G	G/A	G/G	A/G	I/III
B	c.736T>A	A	T	C	A	A	C	C	G	G	A	I
	c.742C>A	G	C	T	C	G	T	G	A	G	G	III
C (homozygote)	c.736T>A	A	T	C	A	A	C	C	G	G	A	I
D	c.736T>A	A	T	C	A	A	C	C	G	G	A	I
	c.742C>A	G	C	T	C	G	T	G	A	G	G	III
E	c.736T>A	A/G	T/C	C/T	A/C	A/G	C/T	C/G	G/A	G/G	A/G	I/III
	c.742C>A	A/G	T/C	C/T	A/C	A/G	C/T	C/G	G/A	G/G	A/G	I/III

Nucleotide numbering starts at +1 corresponding to the A of the ATG initiation codon in the reference sequence AY093498.1 (www.hgvs.org/mutnomen). SNP, single-nucleotide polymorphism.

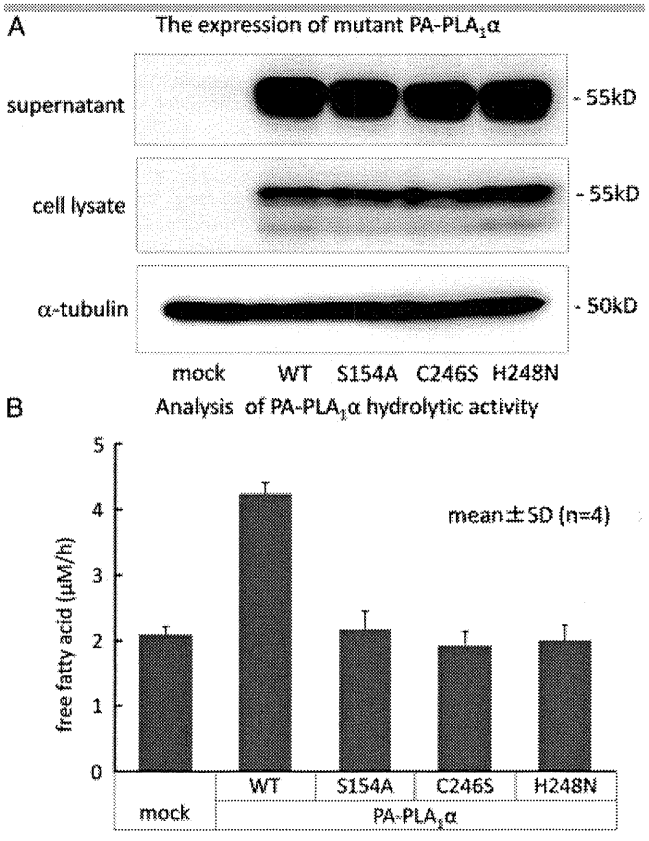

Figure 4. Expression of PA-PLA$_1$α in HEK293 cells and its hydrolytic activity. **A:** Expression of mutant PA-PLA$_1$α in HEK293 cells. HEK293 cells were transfected with wild-type (WT), p.Ser154Ala (S154A), p.Cys246Ser (C246S), and p.His248Asn (H248N) *LIPH* cDNA, and the expression level of PA-PLA$_1$α protein derived from the constructs in cell culture supernatant (upper panel) and cells (middle panel) were evaluated by Western blot. There were no significant differences in PA-PLA$_1$α protein expression levels among cells trasfected with WT, S154A, C246S, and H248N. α-tubulin expression was used as a standard to assess the total amount of proteins from cell lysate loaded on the gel (lower panel). **B:** Because PA-PLA$_1$α hydrolyzes the free fatty acid (FFA) from PA, we monitored the levels FFA to determine whether there is a difference in the PA-PLA$_1$α hydrolytic activity among WT and the three mutants of PA-PLA$_1$α. After 12-hr incubation of the supernatant from HEK293 cells expressing WT, S154A, C246S, or H248N PA-PLA$_1$α, with a medium including 100 μM PA, the levels of FFA hydrolyzed by C246S and H248N mutant PA-PLA$_1$α were significantly lower than that by WT PA-PLA$_1$α and similar to those produced by supernatant from HEK293 cells transfected with control S154A mutant and an empty vector (mock).

quantified using *p*-NPP as a substrate for AP. The free AP-TGFα from the P2Y5 mock transfected (P2Y5-) cells transfected with the WT form of PA-PLA$_1$α was more abundant than that from the P2Y5− cells transfected with empty vector, which indicated that the HEK293 cells had the ability to shed TGFα mediated by intrinsic LPA receptor at some level (Fig. 5A). AP-TGFα release from P2Y5 positive (P2Y5+) cells expressing the WT PA-PLA$_1$α was remarkably increased compared with mock or mutant PA-PLA$_1$α. There were no significant differences between the data obtained with cells expressing the mutants and the empty vector (Fig. 5A). All the cells expressing AP-TGFα responded equally to TPA, confirming that expression of P2Y5 and PA-PLA$_1$α did not affect PKC-dependent AP-TGFα release (Fig. 5B). These data clearly indicated that these mutations resulted in the loss of P2Y5 activation activity of PA-PLA$_1$α.

Discussion

The human *LIPH* gene encodes PA-PLA$_1$α, which is a member of the membrane-associated phosphatidic acid-preferring phospholipase A$_1$α [Hiramatsu et al., 2003; Jin et al., 2002; Sonoda et al., 2002]. Similar to other phospholipase A$_1$, PA-PLA$_1$α has N-terminal domains that are essential for catalytic activity. Three amino acid residues, Ser^{154}, Asp^{178}, and His^{248}, which form the putative catalytic triad, are located in the N-terminal domains [Aoki et al., 2007; Jin et al., 2002; Kubiak et al., 2001; Sonoda et al., 2002] (Fig. 2B). PA-PLA$_1$α has a β9 loop (the 13 amino acids from p.206 to 218) and a short lid domain (the 12 amino acids from p.234 to245), each of which is considered a crucial structure for substrate recognition [Aoki et al., 2007; Carriere et al., 1998; Sonoda et al., 2002]. In addition, well-conserved cysteine residues including Cys^{246}, which form intramolecular disulfide bonds, are in the N-terminal domains.

We performed *DSG4, LIPH*, and *LPAR6* gene mutation analysis and identified two prevalent missense mutations in the *LIPH* gene in the five independent Japanese ARH families. One mutation c.736T>A leads to an amino acid change within conserved cysteine residue that forms intramolecular disulfide bonds on the lid domain (p.Cys246Ser) (Fig. 2). The other mutation c.742C>A results in alteration of one amino acid of the catalytic triad (p.His248Asn) (Fig. 2B). These two residues, Cys^{246} and His^{248}, are highly conserved among *LIPH* of diverse species (Fig. 2A), suggesting that they play a critical role in enzyme activity. We speculate that these mutations drastically affect PA-PLA$_1$α activity.

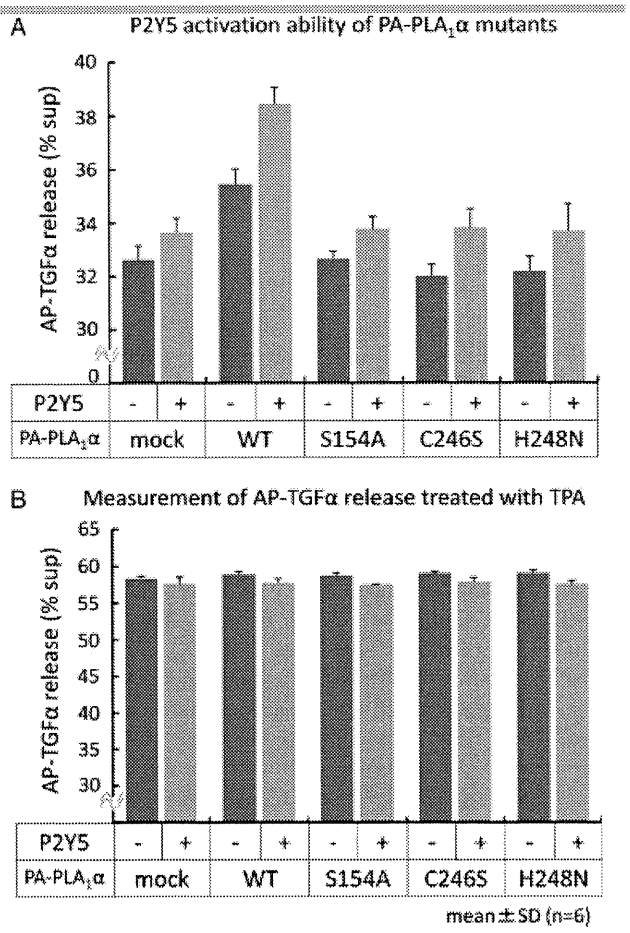

Figure 5. P2Y5 activation ability of PA-PLA$_1$α mutants. To monitor P2Y5 activation level by mutant and wild-type (WT) PA-PLA$_1$α, we used *p*-nitrophenyl phosphate as a substrate for cleavage of AP-TGFα and measured the amount of AP-TGFα released from the HEK293 cells. **A:** The amount of free AP-TGFα produced by P2Y5 mock-transfected (P2Y5−) cells that were also transfected with WT PA-PLA$_1$α is significantly greater than that produced by P2Y5− cells transfected with an empty vector (mock). This indicates that HEK293 cells act to shed AP-TGFα, an activity that might be mediated by intrinsic LPA receptors. The amounts of AP-TGFα released from P2Y5-transfected (P2Y5+) cells expressing p.Ser154Ala (S154A), p.Cys246-Ser (C246S), or p.His248Asn (H248N) mutant PA-PLA$_1$α and P2Y5+ cells transfected with an empty vector (mock) are significantly lower than that from P2Y5+ cells expressing WT PA-PLA$_1$α. **B:** TPA sheds AP-TGFα independently from the P2Y5 pathway. Effects of the TPA-induced shedding of AP-TGFα are similar in all the cells.

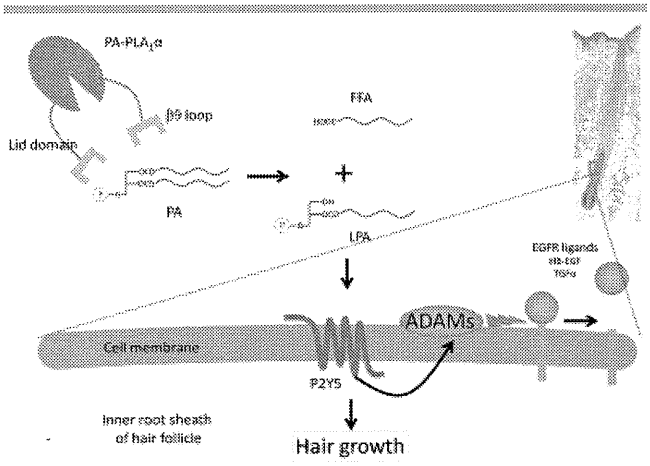

Figure 6. Schematic signaling pathways of LPA produced by PA-PLA$_1$α via the P2Y5 receptor. PA-PLA$_1$α hydrolyzes PA and produces LPA and FFA. LPA works as a ligand for P2Y5, a membrane-bound G-protein-coupled receptor. It has been documented that ADAM activation by P2Y5 results in ectodomain shedding of cell surface proteins including those of the EGF ligand family, such as HB-EGF and TGFα. These signal pathways are speculated to regulate proliferation and differentiation of inner root sheath cells of hair follicles. Abbreviations: PA, phosphatidic acid; FFA, free fatty acid; LPA, 2-acyl lysophosphatidic acid; ADAM, a disintegrin and metalloprotease; EGF, epidermal growth factor; HB-EGF, heparin binding EGF-like growth factor; TGFα, transforming growth factor-α.

So far, 14 *LIPH* gene mutations have been reported, four of which are prevalent [Ali et al., 2007; Horev et al., 2009; Jelani et al., 2008; Kamran-ul-Hassan Naqvi et al., 2009; Kazantseva et al., 2006; Nahum et al., 2009; Naz et al., 2009; Pasternack et al., 2009; Petukhova et al., 2009; Shimomura et al., 2009a,b,c]. One prevalent mutation, 985-bp deletion including exon 4 and the flanking introns, was detected in a large number of ARH patients from two ethnic groups, the Chuvash and Mari, in the Volga–Ural region of Russia [Kazantseva et al., 2006]. The ancestors of the Chuvash population settled in territory occupied by ancestral Mari populations. To determine the frequency of the mutant allele, they tested 2,292 chromosomes in the populations and found the *LIPH* deletion in populations of Chuvash (mutant allele frequency $P = 0.033$) and Mari (mutant allele frequency $P = 0.030$) origin. The mutant allele was restricted to these two populations and was not found in other Finno–Ugric populations or Russian populations from distant geographic regions [Kazantseva et al., 2006].

A deletion mutation exon7_8del has been identified in five consanguineous Pakistani families and 1 Guyanese family [Jelani et al., 2008; Petukhova et al., 2009; Shimomura et al., 2009b, 2009c]. A small deletion mutation 659_660delTA has been identified in several consanguineous Pakistani families and 1 Guyanese family [Jelani et al., 2008; Petukhova et al., 2009; Shimomura et al., 2009b,c]. Both mutations were defined as founder mutations shared in families from Pakistan and Guyana by haplotype analysis using microsatellite markers close to the *LIPH* gene [Jelani et al., 2008; Petukhova et al., 2009; Shimomura et al., 2009b,c]. In fact, these Guyanese families with ARH were descended from people who had come from India about 100 years ago, and it is plausible that both mutations originated from the Indian population [Shimomura et al., 2009c]. However, neither exon7_8del nor 659_660delTA mutations were detected in healthy control individuals of Pakistani origin and their minor allele frequencies were thought to be low in the Pakistani population [Jelani et al., 2008; Shimomura et al., 2009b].

All six of the Japanese ARH patients from the five families in the present study were compound heterozygous for c.736T>A (p.Cys246Ser) and c.742C>A (p.His248Asn) or homozygous for c.736T>A (p.Cys246Ser). c.736T>A (p.Cys246Ser) was found in all five families, and c.742C>A (p.His248Asn) was detected in four of the five families. Most recently, these missense mutations were identified in three Japanese ARH families [Shimomura et al., 2009a]. One family carries two heterozygous missense mutations, c.736T>A and c.742C>A, and the other two families are homozygous for the mutation c.736T>A. Thus, the missense mutations c.736T>A (p.Cys246Ser) and c.742C>A (p.His248Asn) are both suggested to be highly prevalent *LIPH* mutations in the Japanese population. In the previous article, however, screening assays with restriction enzymes excluded the existence of both

mutations in 100 unrelated healthy control individuals (200 alleles) of Japanese origin [Shimomura et al., 2009a]. In this study, in contrast, we used direct sequences and MASA analysis and identified these mutations in four alleles out of 200 unrelated control alleles (100 individuals) (minor allele frequency of c.736T>A, 3/200 $P = 0.015$; c. 742C>A, 1/200 $P = 0.005$; combined genotype, 4/200 $P = 0.020$). In addition, the present haplotype analysis revealed that the mutant alleles with c.736T>A and those with c.742C>A had specific haplotypes, respectively, which suggests that they derive from their own independent founders (Fig. 3, Table 1). From these results, we consider that the *LIPH* mutations c.736T>A (p.Cys246Ser) and c.742C>A (p.His248Asn) are extremely prevalent founder mutations for ARH in the Japanese population.

Previously, several deletion mutations and four missense mutations were reported in the *LIPH* gene [Ali et al., 2007; Horev et al., 2009; Jelani et al., 2008; Kamran-ul-Hassan Naqvi et al., 2009; Kazantseva et al., 2006; Nahum et al., 2009; Naz et al., 2009; Pasternack et al., 2009; Petukhova et al., 2009; Shimomura et al., 2009a,b,c]. In previous cases, ARH patients exhibited wide variability in the hypotrichosis phenotype, although most patients showed wooly hair during early childhood [Shimomura et al., 2009b]. Even ARH patients with identical *LIPH* gene mutations showed a wide variation in phenotype [Shimomura et al., 2009b]. In our cases, all the affected individuals had sparse, curled hair that grew slowly from birth and then stopped growing after reaching a few inches. There are no significant differences in clinical features between families and patients. We cannot exclude the possibility that differences in phenotype will emerge in the future, because our patients were still less than 10 years of age. The clinical features of the five families presented here are similar to those of families with the other mutations in the *LIPH* gene, and no apparent genotype/phenotype correlation was observed between the patients with deletion mutations and those with missense mutations.

PA-PLA$_1\alpha$ hydrolyzes PA and produces LPA and FFA concurrently [Sonoda et al., 2002]. The LPA that is produced by PA-PLA$_1\alpha$ acts as a ligand for P2Y5, one of the G-protein-coupled receptors (GPCRs), which has been identified as another causative gene for human hair growth deficiency [Pasternack et al., 2008; Shimomura et al., 2008]. It has been documented that ADAM activation by GPCRs introduces the ectodomain shedding of cell surface proteins, including the epidermal growth factor (EGF) ligand family whose members include heparin-binding EGF-like growth factor (HB-EGF) and TGFα [Ohtsu et al., 2006] (Fig. 6).

In this study, we performed two different in vitro PA-PLA$_1\alpha$ enzyme activity analyses. One involved analyzing PA-PLA$_1\alpha$ hydrolytic activity by measuring FFA (unpublished data). The p.Cys246Ser and p.His248Asn mutants showed complete abolition of PA-PLA$_1\alpha$ hydrolytic activity, comparable with supernatant of cells transfected with the empty vector only or with the control loss-of-function mutant carrying p.Ser154Ala. The other involved analyzing the P2Y5 activation ability of LPA produced by PA-PLA$_1\alpha$ by assaying free AP-TGFα (unpublished data). In this analysis, the p.Cys246Ser and p.His248Asn mutant PA-PLA$_1\alpha$ had no ability to activate P2Y5. These results clearly indicated that a loss of PA-PLA$_1\alpha$ function leads to defective activation of P2Y5 by LPA, resulting in ARH phenotype in ARH patients with *LIPH* mutations. Thus, complete loss of P2Y5 activation due to reduced LPA is thought to be involved in the pathogenesis of ARH.

While we were preparing the manuscript, Pasternack et al. [2009] reported that PA-PLA$_1\alpha$ derived from mutants with c.403_409 duplication frameshift mutation and in-frame mutations including c.280_369dup and c.527_628del did not show the enzymatic activity of converting PA to LPA in vitro, and that they did not activate P2Y5. The results presented in this study completely agree with their results, although the assay system for enzymatic evaluation and P2Y5 activation used by Pasternack et al. [2009] is quite different from ours. In addition, the affected amino acids in the mutant PA-PLA$_1\alpha$ analyzed in this study were quite different. Interestingly, our in vitro enzyme activity analysis revealed that the present two missense mutations strikingly affected the PA-PLA$_1\alpha$ activity as much as frameshift mutations and large deletion mutations like c.403_409 dup, c.280_369dup, and c.527_628del. These results were consistent with the fact that there is no significant difference in severity of hair loss between the present patients with missense mutations and affected individuals with frameshift mutations or large deletion mutations, c.403_409 dup, c.280_369dup, and c.527_628del. These results clearly indicated that the loss of PA-PLA$_1\alpha$ function caused by the two present mutations leads to defective activation of P2Y5 by LPA and suggest that loss of P2Y5 activation due to reduced LPA is involved in the pathogenesis of ARH.

Acknowledgments

We thank the patients for their generous cooperation and Ms. Akari Nagasaki, Ai Hayakawa, Yuko Hayakawa, and Shizuka Miyakoshi for their technical assistance on this project. This work was supported in part by Grant-in-Aid from the Ministry of Education, Science, Sports, and Culture of Japan to M. Akiyama (Kiban B 20390304) and by a grant from Ministry of Health, Labor and Welfare of Japan (Health and Labor Sciences Research Grants; Research on Intractable Diseases; H21-047) to M. Akiyama.

References

Ali G, Chishti MS, Raza SI, John P, Ahmad W. 2007. A mutation in the lipase H (LIPH) gene underlie autosomal recessive hypotrichosis. Hum Genet 121: 319–325.

Aoki J, Inoue A, Makide K, Saiki N, Arai H. 2007. Structure and function of extracellular phospholipase A1 belonging to the pancreatic lipase gene family. Biochimie 89:197–204.

Barrett JC, Fry B, Maller J, Daly MJ. 2005. Haploview: analysis and visualization of LD and haplotype maps. Bioinformatics 21:263–265.

Carriere F, Withers-Martinez C, van Tilbeurgh H, Roussel A, Cambillau C, Verger R. 1998. Structural basis for the substrate selectivity of pancreatic lipases and some related proteins. Biochim Biophys Acta 1376:417–432.

Hasegawa Y, Takeda S, Ichii S, Koizumi K, Maruyama M, Fujii A, Ohta H, Nakajima T, Okuda M, Baba S, Nakamura Y. 1995. Detection of K-ras mutations in DNAs isolated from feces of patients with colorectal tumors by mutant-allele-specific amplification (MASA). Oncogene 10:1441–1445.

Hiramatsu T, Sonoda H, Takanezawa Y, Morikawa R, Ishida M, Kasahara K, Sanai Y, Taguchi R, Aoki J, Arai H. 2003. Biochemical and molecular characterization of two phosphatidic acid-selective phospholipase A1s, mPA-PLA1alpha and mPA-PLA1beta. J Biol Chem 278:49438–49447.

Horev L, Tosti A, Rosen I, Hershko K, Vincenzi C, Nanova K, Mali A, Potikha T, Zlotogorski A. 2009. Mutations in lipase H cause autosomal recessive hypotrichosis simplex with woolly hair. J Am Acad Dermatol 61:813–818.

Jelani M, Wasif N, Ali G, Chishti M, Ahmad W. 2008. A novel deletion mutation in LIPH gene causes autosomal recessive hypotrichosis (LAH2). Clin Genet 74:184–188.

Jin W, Broedl UC, Monajemi H, Glick JM, Rader DJ. 2002. Lipase H, a new member of the triglyceride lipase family synthesized by the intestine. Genomics 80:268–273.

Kamran-ul-Hassan Naqvi S, Raza SI, Naveed AK, John P, Ahmad W. 2009. A novel deletion mutation in the phospholipase H (LIPH) gene in a consanguineous Pakistani family with autosomal recessive hypotrichosis (LAH2). Br J Dermatol 160:194–196.

Kazantseva A, Goltsov A, Zinchenko R, Grigorenko AP, Abrukova AV, Moliaka YK, Kirillov AG, Guo Z, Lyle S, Ginter EK, Rogaev EI. 2006. Human hair growth

deficiency is linked to a genetic defect in the phospholipase gene LIPH. Science 314:982–985.

Kljuic A, Bazzi H, Sundberg JP, Martinez-Mir A, O'Shaughnessy R, Mahoney MG, Levy M, Montagutelli X, Ahmad W, Aita VM, Gordon D, Uitto J, Whiting D, Ott J, Fischer S, Gilliam TC, Jahoda CA, Morris RJ, Panteleyev AA, Nguyen VT, Christiano AM. 2003. Desmoglein 4 in hair follicle differentiation and epidermal adhesion: evidence from inherited hypotrichosis and acquired pemphigus vulgaris. Cell 113:249–260.

Kubiak RJ, Yue X, Hondal RJ, Mihai C, Tsai MD, Bruzik KS. 2001. Involvement of the Arg-Asp-His catalytic triad in enzymatic cleavage of the phosphodiester bond. Biochemistry 40:5422–5432.

Moss C, Martinez-Mir A, Lam H, Tadin-Strapps M, Kljuic A, Christiano AM. 2004. A recurrent intragenic deletion in the desmoglein 4 gene underlies localized autosomal recessive hypotrichosis. J Invest Dermatol 123:607–610.

Nahum S, Pasternack SM, Pforr J, Indelman M, Wollnik B, Bergman R, Nothen MM, Konig A, Khamaysi Z, Betz RC, Sprecher E. 2009. A large duplication in LIPH underlies autosomal recessive hypotrichosis simplex in four Middle Eastern families. Arch Dermatol Res 301:391–393.

Naz G, Khan B, Ali G, Azeem Z, Wali A, Ansar M, Ahmad W. 2009. Novel missense mutations in lipase H (LIPH) gene causing autosomal recessive hypotrichosis (LAH2). J Dermatol Sci 54:12–16.

Ohtsu H, Dempsey PJ, Eguchi S. 2006. ADAMs as mediators of EGF receptor transactivation by G protein-coupled receptors. Am J Physiol Cell Physiol 291:C1–C10.

Pasternack SM, von Kugelgen I, Aboud KA, Lee YA, Ruschendorf F, Voss K, Hillmer AM, Molderings GJ, Franz T, Ramirez A, Nürnberg P, Nöthen MM, Betz RC. 2008. G protein-coupled receptor P2Y5 and its ligand LPA are involved in maintenance of human hair growth. Nat Genet 40:329–334.

Pasternack SM, von Kugelgen I, Muller M, Oji V, Traupe H, Sprecher E, Nothen MM, Janecke AR, Betz RC. 2009. In vitro analysis of LIPH mutations causing hypotrichosis simplex: evidence confirming the role of lipase H and lysophosphatidic acid in hair growth. J Invest Dermatol 129:2772–2776.

Petukhova L, Shimomura Y, Wajid M, Gorroochurn P, Hodge SE, Christiano AM. 2009. The effect of inbreeding on the distribution of compound heterozygotes: a lesson from Lipase H mutations in autosomal recessive woolly hair/hypotrichosis. Hum Hered 68:117–130.

Rafique MA, Ansar M, Jamal SM, Malik S, Sohail M, Faiyaz-Ul-Haque M, Haque S, Leal SM, Ahmad W. 2003. A locus for hereditary hypotrichosis localized to human chromosome 18q21.1. Eur J Hum Genet 11: 623–628.

Shimomura Y, Ito M, Christiano AM. 2009a. Mutations in the LIPH gene in three Japanese families with autosomal recessive woolly hair/hypotrichosis. J Dermatol Sci 56:205–207.

Shimomura Y, Wajid M, Ishii Y, Shapiro L, Petukhova L, Gordon D, Christiano AM. 2008. Disruption of P2RY5, an orphan G protein-coupled receptor, underlies autosomal recessive woolly hair. Nat Genet 40:335–339.

Shimomura Y, Wajid M, Petukhova L, Shapiro L, Christiano AM. 2009b. Mutations in the lipase H gene underlie autosomal recessive woolly hair/hypotrichosis. J Invest Dermatol 129:622–628.

Shimomura Y, Wajid M, Zlotogorski A, Lee YJ, Rice RH, Christiano AM. 2009c. Founder mutations in the lipase h gene in families with autosomal recessive woolly hair/hypotrichosis. J Invest Dermatol 129:1927–1934.

Sonoda H, Aoki J, Hiramatsu T, Ishida M, Bandoh K, Nagai Y, Taguchi R, Inoue K, Arai H. 2002. A novel phosphatidic acid-selective phospholipase A1 that produces lysophosphatidic acid. J Biol Chem 277:34254–34263.

Tokumaru S, Higashiyama S, Endo T, Nakagawa T, Miyagawa JI, Yamamori K, Hanakawa Y, Ohmoto H, Yoshino K, Shirakata Y, Matsuzawa Y, Hashimoto K, Taniguchi N. 2000. Ectodomain shedding of epidermal growth factor receptor ligands is required for keratinocyte migration in cutaneous wound healing. J Cell Biol 151:209–220.

Wali A, Chishti MS, Ayub M, Yasinzai M, Kafaitullah, Ali G, John P, Ahmad W. 2007. Localization of a novel autosomal recessive hypotrichosis locus (LAH3) to chromosome 13q14.11–q21.32. Clin Genet 72:23–29.

Whittock NV, Bower C. 2003. Genetic evidence for a novel human desmosomal cadherin, desmoglein 4. J Invest Dermatol 120:523–530.

Xu X, Quiros RM, Gattuso P, Ain KB, Prinz RA. 2003. High prevalence of BRAF gene mutation in papillary thyroid carcinomas and thyroid tumor cell lines. Cancer Res 63:4561–4567.

The American Journal of Pathology, Vol. 177, No. 1, July 2010

DOI: 10.2353/ajpath.2010.091120

Epithelial and Mesenchymal Cell Biology

Self-Improvement of Keratinocyte Differentiation Defects During Skin Maturation in ABCA12-Deficient Harlequin Ichthyosis Model Mice

Teruki Yanagi,* Masashi Akiyama,* Hiroshi Nishihara,† Junko Ishikawa,‡ Kaori Sakai,* Yuki Miyamura,* Ayano Naoe,‡ Takashi Kitahara,‡ Shinya Tanaka,§ and Hiroshi Shimizu*

From the Department of Dermatology, Laboratory of Translational Pathology,† the Laboratory of Cancer Research,§ the Department of Pathology, Hokkaido University Graduate School of Medicine, Sapporo; and Tochigi Research Laboratories,‡ Kao Corporation, Ichikai, Haga, Tochigi, Japan*

Harlequin ichthyosis (HI) is caused by loss-of-function mutations in the keratinocyte lipid transporter ABCA12. The patients often die in the first 1 or 2 weeks of life, although HI survivors' phenotypes improve within several weeks after birth. In order to clarify the mechanisms of phenotypic recovery, we studied grafted skin and keratinocytes from *Abca12*-disrupted (*Abca12*$^{-/-}$) mice showing abnormal lipid transport. *Abca12*$^{-/-}$ neonatal epidermis showed significantly reduced total ceramide amounts and aberrant ceramide composition. Immunofluorescence and immunoblotting of *Abca12*$^{-/-}$ neonatal epidermis revealed defective profilaggrin/filaggrin conversion and reduced protein expression of the differentiation-specific molecules, loricrin, kallikrein 5, and transglutaminase 1, although their mRNA expression was up-regulated. In contrast, *Abca12*$^{-/-}$ skin grafts kept in a dry environment exhibited dramatic improvements in all these abnormalities. Increased transepidermal water loss, a parameter representing barrier defect, was remarkably decreased in grafted *Abca12*$^{-/-}$ skin. Ten-passage sub-cultured *Abca12*$^{-/-}$ keratinocytes showed restoration of intact ceramide distribution, differentiation-specific protein expression and profilaggrin/filaggrin conversion, which were defective in primary-cultures. Using cDNA microarray analysis, lipid transporters including four ATP-binding cassette transporters were up-regulated after sub-culture of *Abca12*$^{-/-}$ keratinocytes compared with primary-culture. These results indicate that disrupted keratinocyte differentiation during the fetal development is involved in the pathomechanism of HI and, during maturation, *Abca12*$^{-/-}$ epidermal keratinocytes regain normal differentiation processes. This restoration may account for the skin phenotype improvement observed in HI survivors. *(Am J Pathol 2010, 177:106–118; DOI: 10.2353/ajpath.2010.091120)*

Harlequin ichthyosis (HI) (OMIM 242500) is one of the most severe genetic skin disorders, and its clinical features at birth include severe ectropion, eclabium, flattening of the ears, and large thick plate-like scales over the entire body.[1] Infants affected with HI frequently die within the early neonatal period, although an increasing survival rate for HI newborns has recently been highlighted.[2] In 2005, we and another independent research group identified mutations in the ATP-binding cassette transporter A12 (ABCA12) gene as the cause of HI.[3,4] We previously demonstrated that a severe ABCA12 deficiency causes defective lipid transport in lamellar granules in the upper spinous and granular layer keratinocytes, resulting in malformation of intercellular lipid layers at the granular/cornified layer interface and epidermal lipid barrier disruption resulting in HI phenotype.[3] We recently generated *Abca12*-disrupted (*Abca12*$^{-/-}$) mice by targeting *Abca12*, which closely reproduced the human HI phenotype and died soon after birth.[5] We tried systemic retinoid administration to the pregnant female mice as a form of fetal therapy, although no therapeutic effect was

Supported in part by a grant-in-aid from the Ministry of Education, Science, Sports, and Culture of Japan (Kiban B 20390304: to M.A.), a grant from Ministry of Health, Labor and Welfare of Japan (Health and Labor Sciences Research grants; Research on Intractable Disease: H21–047 and H22-177: to M.A.), a grant from ONO Medical Research Foundation (T.Y.) and a grant from Kanae Foundation for the promotion of Medical Science (T.Y.).

Accepted for publication February 26, 2010.

None of the authors declare any relevant financial relationships.

Supplemental material for this article can be found on *http://ajp.amjpathol.org*.

Address reprint requests to Masashi Akiyama, M.D., Ph.D., or Hiroshi Shimizu, M.D., Ph.D., Department of Dermatology, Hokkaido University Graduate School of Medicine, N15 W7, Kita-ku, Sapporo 060-8638, Japan. E-mail: akiyama@med.hokudai.ac.jp or shimizu@med.hokudai.ac.jp.

obtained in the *Abca12*$^{-/-}$ newborns after treatment.[5] After our publication, Zuo et al[6] also reported another *Abca12* knockout mouse, whose skin showed similar features to our model mice.

Previously, we demonstrated severe skin barrier defects in *Abca12*$^{-/-}$ mice and suggested that "barrier insufficiency" plays an important role in HI phenotype expression.[5] However, "the barrier insufficiency" theory fails to completely explain the pathomechanism of the HI phenotype. HI fetuses show a HI phenotype even *in utero*, where skin barrier protection against a dry environment is not required. In addition, the skin phenotype of HI long-term survivors maintained in a dry environment shows a dramatic improvement within several weeks after birth where they require a normal skin barrier function. Thus, we suspected that other unknown mechanisms are involved in HI and the formation HI survivors' skin phenotypes. To date there have been no reports which have compared the skin phenotypes in fatally affected HI neonates and survivors, and the exact mechanism of HI survivors' skin phenotype improvement has yet to be clarified. Thus, we have carefully analyzed the keratinization process of neonatal versus grafted HI model mice skin and primary versus subcultured *Abca12*$^{-/-}$ keratinocytes instead of human HI neonatal and survivors' skin. Initially, we investigated the distribution and amounts/composition of lipids, and expression of differentiation-specific molecules in neonatal HI model mice skin. Then, we studied the alteration of them in grafted HI model mouse skin transplanted onto severe combined immunodeficient (SCID) mice. In addition, we performed keratinocyte culture experiments including immunostaining and Western blotting using primary/subcultured *Abca12*$^{-/-}$ keratinocytes to confirm the results of the neonatal and grafted skin experiments. Further, we analyzed the whole gene expression profile of primary versus subcultured *Abca12*$^{-/-}$ keratinocytes using cDNA microarray methods. Finally, we conducted therapeutic trials on primary-cultured *Abca12*$^{-/-}$ keratinocytes and grafted HI model mice skin with retinoids.

Materials and Methods

Animals

All animal studies were reviewed and approved by the Animal Use and Care Committee of the Hokkaido University Graduate School of Medicine. C57BL/6 strain mice and SCID mice were purchased from Clea (Tokyo, Japan). All animals used for this study were maintained under pathogen-free conditions.

Antibodies

Rabbit polyclonal affinity purified anti-mouse Abca12 antibody was raised in rabbits using a 14-amino acid sequence synthetic peptide (residues 2581 to 2594) derived from the mouse Abca12 sequence (XM001002308) as the immunogen.[5] The other primary antibodies were rabbit anti-profilaggrin/filaggrin antibody (COVANCE, Princeton, NJ), rabbit anti-involucrin antibody (M-116; Santa Cruz Biotechnology, Santa Cruz, CA), rabbit anti-desmoglein 1 antibody (H-290; Santa Cruz Biotechnology), rabbit anti-mouse loricrin antibody (AF62; COVANCE), rabbit anti-kallikrein 5 antibody (ab7283; Abcam, Cambridge, UK), rabbit anti-glucosylceramide/ceramide antibody (Glycobiotech, Kukels, Germany), and mouse monoclonal anti-β actin antibody (Sigma Chemical Co., St. Louis, MO). Secondary antibodies used in the present study were as follows; Alexa Fluor 488-conjugated donkey anti-rabbit IgG (Invitrogen Corp., Carlsbad, CA), fluorescein isothiocyanate-conjugated goat anti-rabbit IgG (Jackson Immuno Research, West Grove, PA), horseradish peroxidase-conjugated goat anti-rabbit IgG or horseradish peroxidase-conjugated goat anti-mouse IgG (Invitrogen Corp.).

Generation of Abca12$^{-/-}$ *Mouse*

The procedure for generating *Abca12*$^{-/-}$ mice has been previously described.[5] Briefly, we cloned mouse genomic DNA Abca12 fragments from the mouse 129Sv/Ev genomic library (Bacpac Resources Center, Children's Hospital Oakland Research Institute, Oakland, CA). We subcloned a 10.6-kb fragment to make the targeting vector. We inserted the PGK/Neo cassette between 47 bp upstream of the exon 30 and 203 bp downstream of exon 30. We transfected the targeting vector by electroporation into 129Sv/Ev embryonic stem cells, then microinjected the correctly targeted embryonic stem cell line into blastocysts obtained from C57BL/6 mice to generate chimeric mice, which we then mated with C57BL/6 females. We crossed the heterozygotes with C57BL/6 over at least five generations, and then intercrossed them to generate the *Abca12*$^{-/-}$ mice. Genotyping was performed by PCR as described previously.[5]

Establishment of Abca12$^{-/-}$ *Mice Keratinocyte Culture*

Skin samples from *Abca12*$^{-/-}$ and wild-type mice were processed for primary keratinocyte culture, and cells were grown according to standard procedures in CnT-57 medium (Cellntec Advanced Cell Systems, Bern, Switzerland). For differentiation induction, culture medium was switched from CnT-57 medium to CnT-02 medium (Cellntec Advanced Cell Systems) and, 24 hours later, the calcium concentration was changed to 1.2 mmol/L. 48 hours later, we performed extractions of total RNA and protein from cultured cells. We established primary-cultured keratinocytes from two *Abca12*$^{-/-}$ mice and two wild-type mice.

Skin Grafting

In total, ten *Abca12*$^{-/-}$ and three wild-type neonates were sacrificed by anesthesia with ether inhalation, and their dorsal skin excised and transplanted onto SCID mice (Clea). Those skin grafts were fully adapted within 2 weeks after grafting. At 3 weeks after transplantation, the skin grafts were harvested for further analysis.

Extraction of Total RNA and Real-Time Reverse Transcriptase PCR Analysis

We separated the epidermis from whole skin samples of wild and *Abca12−/−* mice by 1 mol/L NaCl in sterile water at 4°C for 2 hours. We isolated total RNA from the epidermis using the Quick Gene RNA Tissue Kit SII (Fujifilm Corp, Tokyo, Japan). We also isolated total RNA from keratinocytes cultured from wild-type and *Abca12−/−* skin using the RNeasy mini kit (Qiagen Corp, Tokyo, Japan). RNA concentration was measured spectrophotometrically and samples were stored at −80°C until use for reverse transcriptase PCR. We reverse-transcribed RNA using Superscript II (Invitrogen Corp.) following the manufacturer's instructions. Complementary DNA samples were analyzed by ABI prism 7000 sequence detection system (Applied Biosystems, Foster City, CA). Primers and probes specific for differentiation-specific protein genes including loricrin, kallikrein 5, transglutaminase 1, involucrin, filaggrin, and control house keeping genes, glyceraldehyde-3-phosphate dehydrogenase (GAPDH), and β-actin, were obtained from Taqman Gene Expression Assay (Applied Biosystems) (Probe ID; Mm01962650_s1, Mm01203811_a1, Mm00498375_a1, Mm00515219_s1, Mm01716522_m1, Mm99999915_g1, and Mm00607939_s1). Differences between the mean CT values of loricrin, kallikrein 5, transglutaminase 1, involucrin, filaggrin and those of GAPDH or β-actin were calculated as: ΔCT*Abca12−/−* mice = CTloricrin (or other keratinization markers) − CTGAPDH (or other house keeping genes) and those of ΔCT for the *Abca12+/+* asΔCT calibrator = CTloricrin (or other keratinization markers) − CTGAPDH (or other house keeping genes).

We could obtain the similar results from GAPDH and β-actin standard, thus we described the results of GAPDH standard in the present study. Final results for *Abca12*$^{-/-}$ mouse samples/wild-type mouse samples (%) were determined by $2^{-(}$ΔCTAbca12−/− sample − ΔCTcalibrator). We measured mRNA levels five times for each clones. Using similar methods, we quantitatively analyzed these differentiation-specific mRNA expression levels in the primary/subcultured keratinocytes from *Abca12*$^{-/-}$ and wild-type mice.

Western Blotting

We separated the epidermis from whole skin samples of wild and *Abca12*$^{-/-}$ mice by 1mol/L NaCl in sterile water at 4°C for 2 hours. For Western blotting, we used epidermal homogenates and proteins extracted from cultured keratinocytes prepared with radioimmunoprecipitation assay (RIPA) buffer comprising 50 mmol/L Tris-HCl, pH7.5, 150 mmol/L NaCl, 1% Nonidet P-40, 0.5% deoxycholate, 0.1% SDS, and Roche protease cocktail tablet (Roche, Basel, Switzerland). Protein concentrations were measured using Micro BCA protein assay kit (Thermo Scientific, Rockford, IL). Protein concentration of the samples for western blotting was from 1 to 2 μg/μl. The 20 μg protein loading per single lane was separated by a 5 to 20% gradient gel SDS-polyacrylamide gel and transferred to polyvinylidene difluoride membranes. Membrane blocking and incubation with antibodies were performed in Tris-buffered saline with 2% nonfat dry milk. Signals were revealed with chemiluminescence reagents and photographed by LAS-1000 mini (Fujifilm Corp, Tokyo, Japan). We also confirmed the loading protein dose by β-actin antibody staining as internal protein control. For analysis of filaggrin solubility and processing, epidermal lysates were prepared with RIPA buffer. Samples of precipitated proteins in the RIPA buffer were solubilized again in 8 mol/L urea before boiling in reducing SDS loading buffer.

Light Microscopy and Immunofluorescence Analysis

For light microscopy, we harvested the newborn pups' skin and the grafted skin, and fixed them for 24 hours in 10% neutral buffered formalin, dehydrated them in graded ethanol, and embedded them in paraffin. We cut 4-μm sections and stained them with H&E. For immunohistochemistry, the tissue samples were embedded in optimal cutting temperature compound (Sakura Finetechnical Corp., Tokyo, Japan). Frozen tissue sections were cut at a thickness of 5 μm. The sections were blocked with 1% bovine serum albumin (BSA) in PBS for 30 minutes at room temperature, and incubated in primary antibody solution in blocking buffer for 30 minutes at 37°C. Fluorescent labeling was performed with secondary antibodies, followed by propidium iodide (Sigma Chemical Co.) for 5 minutes at room temperature to counterstain nuclei. The stained samples were observed under an Olympus Fluoview confocal laser-scanning microscope (Olympus, Tokyo, Japan).

In Situ *Transglutaminase Activity*

The procedure for *in situ* transglutaminase 1 activity assay has been previously described.[7,8] In brief, unfixed cryosections of 5 μm were blocked with 100 mmol/L Tris-HCl pH7.4, 1% BSA for 30 minutes, and then incubated with 100 mmol/L Tri-HCl pH7.4, 5 mmol/L $CaCl_2$, 12 μmol/L monodansylcadaverine (Sigma) for 1 hour to detect transglutaminase 1 activity. For negative controls, EDTA was added to the monodansylcadaverine solution to a final concentration of 20 mmol/L. After stopping the transglutaminase 1 reaction with 10 mmol/L EDTA in PBS, sections were incubated with rabbit anti-dansyl antibody (Invitrogen Corp.) in 12% BSA/PBS for 3 hours. Sections were then incubated with fluorescein isothiocyanate-conjugated goat anti-rabbit antibody in 12% BSA/PBS for 30 minutes. Nuclei were counterstained by propidium iodide. The stained samples were observed under an Olympus Fluoview confocal laser-scanning microscope (Olympus).

Immunofluorescence Labeling of Cultured Cells

Immunofluorescence labeling of cultured cells was performed as previously described.[5] Briefly, primary/subcultured keratinocytes were fixed in 4% paraformaldehyde for 15 minutes and permeabilized with 0.1% Triton X-100 for 15 minutes at room temperature. Keratinocytes were blocked with 1% BSA in PBS for 30 minutes at room temperature,